Microbiology of fly ash-acid mine drainage co-disposal processes

By

Eloise M. R. Kuhn

Submitted in fulfilment of the requirements for the degree of Magister Scientiae (M.Sc.) in the Department of Biotechnology, University of the Western Cape.

Supervisor: Prof. D.A. Cowan

November 2005

Abstract

The waste products acid mine drainage (AMD), formed during coal mining and fly ash (FA) from coal burning power generation, pose substantial environmental and economic problems for South Africa. Eskom has developed a remediation system employing alkaline FA to neutralize and precipitate heavy metals from toxic acidic AMD streams. The aim of this study was to assess the microbial diversity in and microbial impact on this remediation system. The total microbial diversity was assessed by well-established molecular phylogenetic analyses using 16S rDNA gene sequences. The results obtained from the AMD confirmed the presence of acidophilic organisms, such as *Acidithiobacillus ferrooxidans* (*At. ferrooxidans*). After co-disposal of FA and AMD, microbial cell growth was not detected and microbial genomic DNA could not be extracted. The absence of microbial communities in the co-disposal phase is beneficial to the continuation of the development of such a co-disposal process. Results of this project will assist in the effective implementation of FA-AMD co-disposal systems, which may improve water quality in effected regions of South-Africa.

Keywords: Acid mine drainage, acidophiles, *Acidithiobacillus ferrooxidans*, coal mining, co-disposal, fly ash, neutralization, remediation system, waste management.

Declaration

I declare that **Microbiology of fly ash-acid mine drainage co-disposal processes** is my own work, that it has not been submitted for any degree or examination in any other university, and that all the sources I have used or quoted have been indicated and acknowledged by complete references.

Miss. Eloise Kuhn November 2005

_____

Acknowledgements

I would like to give recognition to the following people who helped in making the project a success:

- ✓ Firstly to **God**, for providing me with strength throughout this project.
- ✓ **Family** and **friends**, for their love, support and understanding throughout my studies.
- ✓ **Prof. Don Cowan**, my research supervisor, for his support and guidance.
- ✓ **Dr. Carola van IJperen**, my co-supervisor, for her assistance and motivation.
- ✓ Members of the **ARCAM Laboratory**, for their technical support and encouraging words.
- ✓ **Ms Damini Surender** at the Eskom-Resources and Strategy Division, Johannesburg, South Africa, for her assistance with the collection and preparation of the samples.
- ✓ **The Water Research Commission**, for providing the project (project number: 1549).
- ✓ **The National Research Foundation**, for funding and financial support.

List of Abbreviations

ALD: anoxic limestone drains

AMD: acid mine drainage

APS: alkalinity producing systems

ARCAM: Advanced Research Centre for Applied Microbiology

ARDRA: amplified rDNA restriction analysis

At. ferrooxidans: *Acidithiobacillus ferrooxidans*

BLAST: basic local alignment sequencing tool

bp: base pairs

cm: centimetres

CTAB: cetyltrimethylammonium bromide

DGGE: denaturing gradient gel electrophoresis

DNA: deoxyribonucleic acid

DTT: dithiothreitol

EC: electrical conductivity

E. coli: *Escherichia coli*

EDTA: ethylenediaminetetra-acetate

Eskom: electricity supply commission: A South African electricity public utility company

FA: fly ash

IPTG: isopropyl-beta-D-thiogalactopyranoside

g: gram

GenBank: nucleotide sequence database

k: kilo

kb: kilobase

L: liter

LB: Luria Bertani

M: molar

m: milli

min: minute

mmst: million short tons

s: second

n: nano

ºC: degrees Celsius

OPC: open limestone channels

PCR: polymerase chain reaction

PVPP: polyvinylpolypyrrolidone

rDNA: ribosomal deoxyribonucleic acid

rpm: rates per minute

SA: South Africa

SDS: sodium dodecyl sulfate

TBE: Tris-Borate-EDTA electrophoresis buffer

TDS: total dissolved solids

TE: Tris-EDTA buffer

Tris: 2-amino-2 (hydroxymethyl) 1,-3-propanediol

UV: ultra violet

V: volts

VBNC: viable but non-culturable

w/v: weight per volume

X-gal: 5-bromo-4-chloro-3-indolyl-beta-D-galactopyranoside

α: alpha

β: beta

γ: gamma

λ: lambda

μ: micro

List of Figures

List of Tables

Table of Contents

Chapter 1
Literature Review

1.1. INTRODUCTION

Coal provides one of the most important natural sources of energy. In South Africa (SA) approximately half of the coal mined is used to produce energy, a quarter to produce synthetic liquid fuels and another quarter used directly in industry and in homes (South Africa Country Analysis Briefs, 2005). Although coal mining is of importance, it presents a number of environmental problems worldwide, including the production of fly ash (FA) and acid mine drainage (AMD). The disposal of FA in dams or heaps presents a huge problem due to the alkalinity (pH >12) and chemical characteristics of FA. Environmental waters polluted with AMD are highly acidic (pH 2.3 - 6.5) and typically red in color (shown in Fig. 1.1).

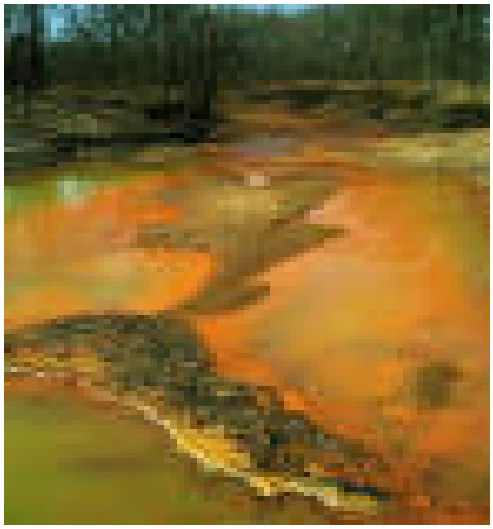

Figure 1.1. Surface waters polluted with AMD have a typical red color.

Eskom has recently developed a pilot remediation system employing FA to neutralize and precipitate metal sulfates from toxic AMD streams. These two waste streams, FA and AMD, have the capacity to neutralize each other through co-disposal. Such a system contains five discrete physical phases: AMD, FA, FA-AMD mixing phase, precipitated Ca/Fe-SO_4- silicate solid phase and a clarified effluent water phase.

1.2. COAL

1.2.1. Definition and origin of Coal

Coal is a natural dark brown to black graphite-like fuel substance of plant origin. It is found in underground seams and is largely composed of amorphous carbon with various organic and some inorganic compounds (The American Heritage® Dictionary, 2000). Coal can be found as carbonized fibers, stems, leaves and seeds of plants embedded in clays, sandstones, or limestones. The coal is removed by surface mining or underground mining methods (The Columbia Encyclopedia, 2001).

1.2.2. Coal Mining in South Africa

Coal is the primary fuel produced and consumed in SA (South Africa Country Analysis Briefs, 2005). The main coalfields in SA are the Witbank, Highveld and Eastern Transvaal (shown in Fig. 1.2; Somerset, 2003).

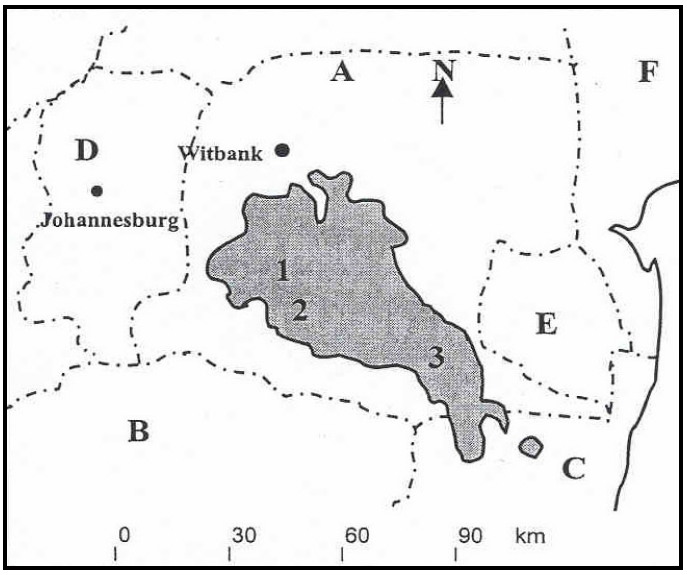

Figure 1.2. Location of coalfields in SA. 1 represents the Witbank coalfield; 2, Highveld coalfield and 3, Eastern Transvaal coalfield. Geographical locations are indicated alphabetically, A represents Mpumalanga -; B, Free State -; C, KwaZulu Natal -; D, Gauteng -; E, Swaziland - and F, Mozambique (Somerset, 2003).

In 2002, SA produced 245.3 million short tons (mmst) of coal, making it the world's sixth largest coal producer (South Africa Country Analysis Briefs, 2005). Although only one-third of coal produced in SA is exported, coal exports provide the country's second largest foreign exchange income. Coal is primarily exported to the European Union and East Asia. In 2002, SA was the world's third largest coal net exporter, exporting 73.7 mmst per annum (South Africa Country Analysis Briefs, 2005).

In SA, coal-fired power stations are usually close to the coalfields. 90% of the electricity supplied by Eskom is generated through coal-fired power stations. The major Eskom coal-fired power stations are shown in Fig. 1.3 (Somerset, 2003).

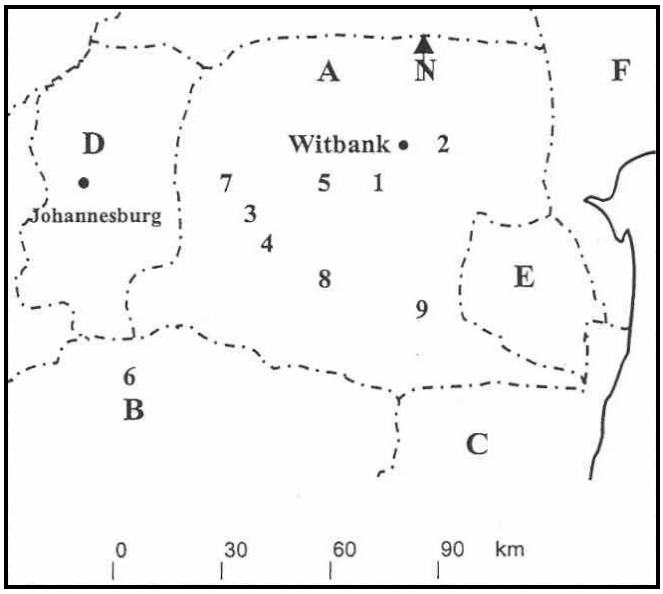

Figure 1.3. Location of the major Eskom coal-fired power stations. 1 represents Hendrina -; 2, Arnot -; 3, Kriel -; 4, Matla -; 5, Duvha -; 6, Lethabo -; 7, Kendal -; 8, Tutuka – and 9, Majuba power stations. Geographical locations are indicated alphabetically, A represents Mpumalanga -; B, Free State -; C, KwaZulu Natal -; D, Gauteng -; E, Swaziland - and F, Mozambique (Somerset, 2003).

1.2.3. Impact of Coal Mining on the environment

The negative impact of coal mining on the environment is of great concern. Mining disturbs geological formations as well as natural systems and processes. These disturbances may cause aquatic and terrestrial pollution (Costello, 2003; Somerset 2003).

The most severe and common problem caused by coal mining is water pollution, caused by heavy metal contaminated water flowing from coal mines. The impact of AMD on the environment includes the damaging of aquatic resources, inhibition of terrestrial and wetland plant growth, contamination of groundwater, increased water treatment costs and damage to concrete and metal structures (Fripp *et al*., 2000). Coal-fired power stations

also have a negative effect on the environment through the production of the waste product, FA.

1.3. FLY ASH (FA)

1.3.1. Definition of FA

FA is a by-product of coal combustion and can be collected from the flue gas steam. The main component of FA is silicon dioxide (SiO_2), although several other oxides (e.g., Al_2O_3, Fe_2O_3, CaO, MgO) are typically present (Czurda and Haus, 2001; Styszko-Grochowiak *et al*., 2004).

1.3.2. Morphology of FA

FA is mostly spherical ferro-alumino silicates with a high surface area and a small particle size (20 – 80 μm) (Gitari *et al*., 2003; Styszko-Grochowiak *et al*., 2004).

1.3.3. Chemistry of FA

The principle elements found in FA are iron (Fe), aluminium (Al), silicon (Si), calcium (Ca), potassium (K), sodium (Na) and titanium (Ti). The most common compounds found in FA are quartz (SiO_2), mullite ($Al_6Si_2O_{13}$), hematite (Fe_2O_3), magnetite (Fe_3O_4) and a small portion of unburned coal. Anhydrite ($CaSO_4$), lime (CaO) and periclase (MgO) can also be found in FA (Petrik *et al*., 2003). FA is highly alkaline and high concentrations of potentially toxic elements are present. The high alkalinities of FA are

due to lime on the surface of the spherules, which originates from the decarbonation of limestone impurities in the coal (The Water Wheel, 2003).

1.3.4. Impact of FA on the environment

Coal FA, which originates from coal combustion, is commonly disposed in coal refuse piles and mine spoil heaps. FA disposal has various effects on both the terrestrial and aquatic ecosystems (Somerset, 2003). In terrestrial ecosystems potentially toxic elements drain into the soil and groundwater. This then effects the surrounding vegetation by reducing plant growth and changing the elemental composition of the soil. It also increases the mobility and accumulation of the potentially toxic and harmful elements throughout the food chain. In aquatic ecosystems the following changes occur; change in water chemistry, pH and change in the concentrations of potentially toxic elements (Somerset, 2003).

1.4. ACID MINE DRAINAGE

1.4.1. Definition of AMD

AMD is defined as drainage flowing from or obtained from surface mining, deep mining or coal refuse piles. The drainage is usually highly acidic (pH 2.3 – 6.5) and contains elevated levels of dissolved metals, including iron, manganese and aluminium (Johnson, 1995). The most dominant metal present in AMD is iron, which may be present in ferrous and ferric forms. In the case of extremely AMD water (pH 2.3 - 4), ferric iron present at a concentration of approximately 650 mg/l colors the water typically red, while in streams

with a higher pH (pH 5 - 6.5), orange-yellow ferric iron-rich (±160 mg/l) sediments ("yellow boy") are present (Johnson and Hallberg, 2003).

1.4.2. Formation of AMD

AMD is formed by a series of geo-chemical and microbial reactions that occur when sulfide minerals (produced during coal mining) are exposed to oxygen, in contact with water. Oxidation of sulfide minerals occurs primarily via reactions mediated by microorganisms. Iron and sulfur are oxidized to ferric iron and sulfate, respectively, and during the oxidation process hydrogen ions are produced (Johnson, 1995).

1.4.3. Chemistry of AMD

The formation of AMD from pyrite can be represented in three basic chemical reactions, pyrite oxidation, ferrous oxidation and iron hydrolysis. Pyrite (FeS_2) is the dominant form of inorganic sulfur in coal. Additionally, an alternative pyrite oxidation may take place (Hallberg and Johnson, 2003). During pyrite oxidation sulfur is oxidized to sulfate and ferric iron is released (equation 1). Two moles of protons are generated for each mole of pyrite oxidized.

Pyrite Oxidation: $4\ FeS_2 + 15\ O_2 + 14\ H_2O \rightarrow 4\ Fe(OH)_3\ (s) \downarrow + 8\ H_2SO_4$ (1)

Pyrite + Oxygen + Water → Ferric Hydroxide + Sulfuric Acid

The second reaction converts ferrous iron into ferric iron (equation 2). This conversion consumes one mole of protons and the reaction rate is pH dependent.

Ferrous Oxidation: $4\ Fe^{2+} + O_2 + 4\ H^+ \rightarrow 4\ Fe^{3+} + 2\ H_2O$ (2)

Ferrous Iron + Oxygen + Protons → Ferric Iron + Water

The final step of the chemical pathway is the hydrolysis of iron (equation 3). Three moles of protons are generated with the formation of a ferric hydroxide precipitate (solid), which is pH dependent.

Iron Hydrolysis: $4\ Fe^{3+} + 12\ H_2O \rightarrow 4\ Fe(OH)_3(s) \downarrow + 12\ H^+$ (3)

Ferric Iron +Water → Ferric Hydroxide + Protons

Additionally, the oxidation of pyrite can also occur by the reduction of ferric iron (equation 4). This reaction takes place very rapidly and continues until either ferric iron or pyrite is depleted. During this reaction iron is the oxidizing agent.

Pyrite Oxidation: $FeS_2 + 14\ Fe^{3+} + 8\ H_2O \rightarrow 15\ Fe^{2+} + 2\ SO_4^{2-} + 16\ H^+$ (4)

Pyrite + Ferric Iron + Water → Ferrous Iron + Sulfate + Protons

1.4.4. Microbiology of AMD

All bacterial species have a definite pH growth range and pH growth optimum. Acidophiles have their growth optimum between pH 0 and pH 5.5 (Prescott *et al*., 1999). Bacterial death might occur when the internal pH drops much below 5.0 to 5.5, because changes in the external pH can alter the ionization of nutrient molecules and then therefore reduce their availability to the organism. However, there are some microorganisms which can survive extreme acidic environments. These microorganisms

frequently change the pH of their own habitat by producing acidic metabolic waste products.

1.4.4.1. Microbial diversity of organisms in AMD

A diversity of organisms has been detected in AMD. Data on eukaryotes and archaea are limited. Eukaryotes isolated from AMD sites include organisms able to graze on mineral-oxidizing acidophilic bacteria, including ciliates belonging to the genus *Cinetochilium*, an amoeba related to *Vahlkampfia* spp. and three flagellates (*Eutreptial* spp.) (Johnson and Rang, 1993; Baker and Banfield, 2003). Metabolically active protists has been found in Richmond Mine biofilms (pH 0.5 – 2.0) and a diverse community eukarya (including alga) was recovered from the Rio Tinto river (pH 2), Spain. Relatively few archaeal taxa have been identified in AMD. These include members of the Thermoplasmatales and Sulfolobales lineages. *Metallosphaera prunae*, a member of the Sulfolobales, has been detected in AMD environments. There are two other members of the Sulfolobales genera, *Acidianus* and *Sulfolobus*, which have only been found in geothermal acidic environments (Baker and Banfield, 2003). Another member of the *archaea* genus is Ferroplasma, which was found in acidophilic biofilms from the Richmond mine at Iron Mountain, California (Tyson *et al.*, 2004; Ram *et al.*, 2005) Bacteria including Proteobacteria, Nitrospira, Firmicutes, and Acidobacteria dominate the microbial populations in AMD (Baker and Banfield, 2003).

Proteobacteria of AMD are divided into three groups, γ-; α-; and β-proteobacteria. The most common proteobacteria are *Acidithiobacillus* species (formally *Thiobacillus*; Kelly

and Wood, 2000), and is characterized as a mesophilic member of the γ-proteobacteria. Six species of heterotrophic α-proteobacteria of the genus *Acidiphilum* have been found (Baker and Banfield, 2003).

Isolates of *Leptospirillum*, a common Nitrospira, cluster within one of three phylogenetically distinct groups, I; II; and III (Bond *et al*., 2000). Two species have been named: *L. ferrooxidans* (group I; Hippe, 2000) and *L. ferriphilum* (group II; Coram and Rawlings, 2002). *Leptospirillum ferrooxidans*-group organisms are commonly detected in AMD and bioleaching systems (Baker and Banfield, 2003). The isolate *Leptospirillum ferrodiazotrophum* is a member of Leptospirillum group III. These groups of organisms have the ability to carry out nitrogen fixation (Tyson *et al.*, 2005).

Three distinct groups of AMD organisms fall within the Firmicutes division. These include *Acidimicrobium ferrooxidans*, *Ferromicrobium acidophilus* and the low G+C Gram-positive *Sulfobacillus* spp. (Baker and Banfield, 2003).

One of the first two metagenome sequencing projects included the sequencing of total DNA from a natural acidophilic biofilm. Reconstruction of near-complete genomes of Leptospirillum group II and Ferroplasma type II, were reported (Tyson *et al.*, 2005).

Acidithiobacillus ferrooxidans

Acidithiobacillus grows in soil, aquatic habitats and reduced inorganic sulfur compounds. This species is metabolically flexible and uses ferrous iron and reduced inorganic sulfur

compounds as an electron donor, to produce ferric iron and sulfuric acid (Prescott *et al.*, 1999). *At. ferrooxidans* is a moderately thermophilic (optimum growth temperature 45°C), gram-negative, chemoautotrophic, sulfur-oxidizing acidophilic bacterium (Razzel and Trussel, 1963; Blake *et al*., 1994; Harahuc *et al*., 2000). The bacterium, previously called *Thiobacillus ferrooxidans*, has been renamed because the genus *Thiobacillus* included a collection of bacteria belonging to the α-; β-; and γ-subclasses of *Proteobacteria* (Kelly and Wood, 2000). *At. ferrooxidans* is of great practical importance due to the extensive acid and metal pollution generated when this species releases metals from mine waters (Prescott *et al.*, 1999).

1.4.4.2. Metabolism of Pyrite

In AMD there are many mineral-degrading acidophiles involved in the metabolism of pyrite. The mineral degrading acidophiles groups into one of six groups (Table 1.1).

The metabolic pathways involved in pyrite metabolism are pyrite dissolution, iron oxidation, iron reduction and sulfur oxidation.

Table 1.1. Mineral-degrading acidophiles involved in pyrite metabolism (Adapted from Johnson and Hallberg, 2003).

Mineral-degrading acidophiles	Thermal classification	Phylogenetic affiliation
Iron-oxidizers		
Leptospirillum ferrooxidans	Mesophile	Nitrospira
L. ferriphilum	Mesophile	Nitrospira
L. thermoferrooxidans	Moderate Thermophile	Nitrospira
Ferroplasma acidiphilum	Mesophile	Thermoplasmales
Sulfur-oxidizers		
At. thiooxidans	Mesophile	β/γ – Proteobacteria
At. caldus	Moderate Thermophile	β/γ – Proteobacteria
Sulfolobus spp.	Extreme Thermophile	Sulfolobales
Iron- and sulphur-oxidizers		
At. ferrooxidans	Mesophile	β/γ – Proteobacteria
Acidianus spp.	Extreme Thermophile	Sulfolobales
Sulfolobus metallicus	Extreme Thermophile	Sulfolobales
Iron-reducers		
Acidiphilium spp.	Mesophile	α – Proteobacteria
Iron-oxidizers/reducers		
Acidimicrobium ferrooxidans	Mesophile	Actinobacteria
Iron-oxidizers/reducers and sulphur-oxidizers		
Sulfobacillus spp.	Mesophile and Moderate Thermophile	Firmicutes

Pyrite Dissolution

The oxidation of pyrite by microorganisms has important economic and environmental consequences. Pyrite oxidation can have a positive as well as a negative effect on the environment. Acidic ferric sulfate, resulting from pyrite oxidation, assists in the commercial recovery of copper and uranium from wastes and ores (Bruynesteyn**,** 1989; Olson, 1991). When pyrite oxidation is not controlled in active or abandoned coal and metal mines, it leads to AMD (Singer and Stumm, 1970; Olson, 1991). The rate at which

pyrite is oxidised is influenced by the supply of oxidant to the mineral surface. Typical oxidants are oxygen and ferric ions (Baker and Banfield, 2003). The oxidation of pyrite leads to the formation of ferric iron (Madigan *et al*., 2000). The dominant pathway for pyrite oxidation is shown in equation 5:

$$14\ Fe^{2+} + 3.5\ O_2 + 14\ H^+ \rightarrow 14\ Fe^{3+} + 7\ H_2O \quad (5)$$

The rate of the reaction in equation 5 may limit the rate of AMD generation, because the oxidation of ferrous iron by O_2 at low pH is slow (Baker and Banfield, 2003).

This reaction is typically followed by the reduction of ferric iron by sulfide (equation 6):

$$FeS_2 + 14\ Fe^{3+} + 8\ H_2O \rightarrow 15\ Fe^{2+} + 2\ SO_4^{2-} + 16\ H^+ \quad (6)$$

There are direct and indirect mechanisms by which metal-mobilizing acidophilic bacteria degrade pyrite (shown in Fig. 1.4). In the direct mechanism, microorganisms attach to mineral sulfides. Once attached, oxidation of both iron and sulfur causes the dissolution of the mineral (FeS_2). This contributes to the development of characteristic corrosion patterns. During the indirect mechanism sulfides are chemically oxidized by soluble ferric iron (Fe^{3+}), which is reduced to ferrous (Fe^{2+}). Ferric iron is regenerated by acidophilic iron-oxidizing bacteria, thus allowing sulfide mineral (FeS_2) oxidation to occur (Mustin *et al*., 1992; Johnson, 1995; Bacelar-Nicolau and Johnson, 1999). Rawlings, 2002, summarizes more recent studies of the direct and indirect mechanism of pyrite oxidation.

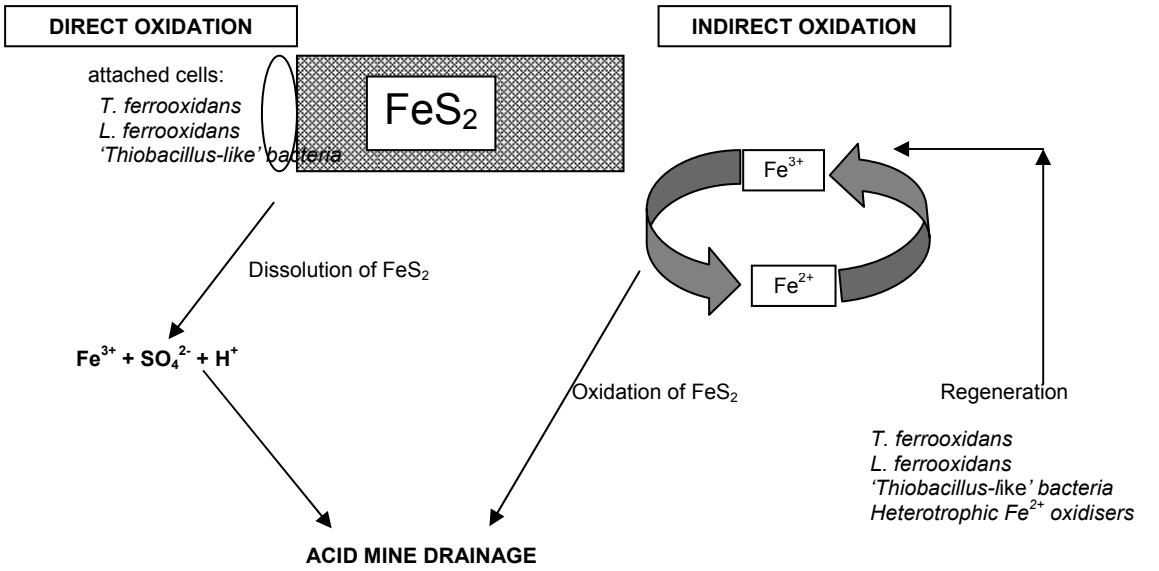

Figure 1.4. Bacterial oxidation of pyrite (FeS_2) by the 'direct' and 'indirect' pathways (Johnson, 1995).

The most common pyrite-oxidizing bacterium is *At. ferrooxidans*. The rate of pyrite oxidation by *At. ferrooxidans* is determined by the levels of soluble iron (Olson, 1991). It also involves chemical oxidation by ferric ions produced by the bacteria (Keller and Murr**,** 1982; Mustin *et al*., 1992). Studies with and without *At. ferrooxidans* show that the rate of pyrite dissolution was lower when *At. ferrooxidans*, was not present at the same ferric and ferrous concentrations (Fowler *et al*., 1999).

Iron Oxidation

The oxidation of iron from the ferrous to the ferric state has a limited energetic yield requiring iron bacteria to oxidize large amounts of iron in order to grow. At neutral pH ferrous iron oxidizes non-biologically to the ferric state and is stable under anaerobic conditions. Ferric iron forms insoluble ferric hydroxide [$Fe(OH)_3$] precipitates in water, called "yellow boy", which forms part of AMD (Madigan *et al*., 2000).

At. ferrooxidans is the best studied iron-oxidizing bacteria and is able to grow autotrophically. At low pH environments *At. ferrooxidans* oxidizes ferrous iron. There is a large proton gradient across the membrane of *At. ferrooxidans*, caused by the different pH of the periplasm (pH 1 – 2) and the cytoplasm (pH 5.5 – 6), which is maintained by ATPase generated protons. Water is produced when electrons travel via a short electron transport chain and O_2 is reduced. The proton motive force across the cytoplasmic membrane synthesizes ATP (Schippers and Sand, 1999; Rohwerder et al., 2003). This can only occur when *At. ferrooxidans* has iron available (shown in Fig. 1.5; Madigan *et al*., 2000).

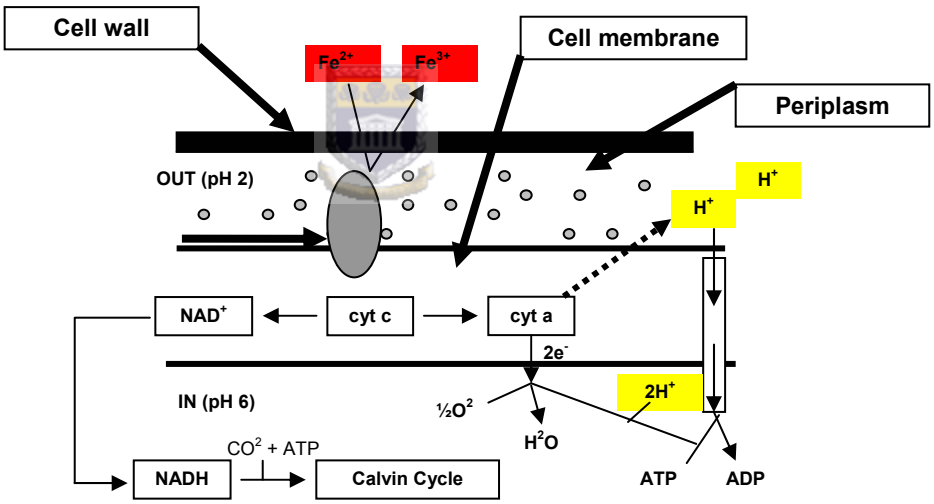

Figure 1.5. Electron flow during Fe^{2+} oxidation by the acidophile *At. ferrooxidans* (Adapted from Madigan *et al*., 2000).

Iron Reduction

Certain bacteria have the ability to reduce ferric iron to ferrous iron. High concentrations of iron are very common in AMD, because both ferric (Fe^{3+}) and ferrous iron (Fe^{2+}) are

very soluble at a pH lower than 2.5 (Baker and Banfield, 2003). This phenomenon has been observed in neutrophilic, heterotrophic bacteria, as well as in some acidophilic chemolithotrophs, including *Thiobacillus thiooxidans*. *At. ferrooxidans* can reduce ferric iron either anaerobically or aerobically (Sand, 1989; Johnson and McGinnes, 1991), a process which involves the enzyme, sulfur-ferric ion oxidoreductase (Sugio *et al*., 1990; Johnson and McGinnes, 1991).

Sulfur Oxidation

Sulfur compounds used as electron donors are hydrogen sulfide (H_2S), elemental sulfur (S^0), thiosulfate ($S_2O_3^{2-}$) and other reduced inorganic sulfur compounds (e.g., tetrathionate). In the presence of oxygen, elemental sulfur is chemically stable, but is oxidized rapidly in the presence of sulfur-oxidizing bacteria such as *At. ferrooxidans*. The oxidation of elemental sulfur releases sulfate and hydrogen ions, resulting in a lowering of the pH. During oxidation sulfide is oxidized to sulfite, which can then be oxidized to sulfate (Madigan *et al*., 2000).

1.5. COAL BY-PRODUCT WASTE MANAGEMENT

Both the by-products of coal mining and coal combustion create problematic wastes, AMD and FA. There are various treatments available for AMD but FA is usually disposed of as a semi-liquid to a dam site, where it solidifies and weathers (Styszko-Grochowiak *et al.*, 2004).

1.5.1. AMD Treatments

AMD treatments can be divided into two categories, active and passive. Active treatment involves chemicals, while passive treatment involves biological processes.

1.5.1.1. Active Treatment

Active treatment of AMD involves the addition of chemicals (Table 2) which raise the pH and cause acid-soluble metals to form insoluble complexes and precipitates. This system is expensive due to the purchase value of the chemicals and the need for disposal of the solid residues produced (Jage *et al*., 2001).

The choice of chemical additive depends on factors such as the acidity level, the types and concentrations of the metals present in the AMD, flow rate, final water quality desired, and the risk factors such as chemical toxicity (Skousen, 1997).

Table 1.2. Chemical compounds used in AMD treatment (Jage *et al*., 2001).

Common Name	**Chemical Name**
Limestone	Calcium Carbonate
Hydrated Lime	Calcium Hydroxide
Pebble Quicklime	Calcium Oxide
Soda Ash	Sodium Carbonate
Caustic Soda	Sodium Hydroxide
Ammonia	Anhydrous Ammonia

Limestone is the most commonly used chemical in AMD treatment due to its relatively low cost, safety and ease of handling. Hydrated lime is also commonly used.

1.5.1.2. Passive Treatment

Active treatment of AMD over long periods is very expensive. Passive treatment of AMD has the advantage of using naturally occurring chemical and biological processes (Jage *et al*., 2001). There are six primary passive technologies (Fig. 1.6; Skousen, 1997).

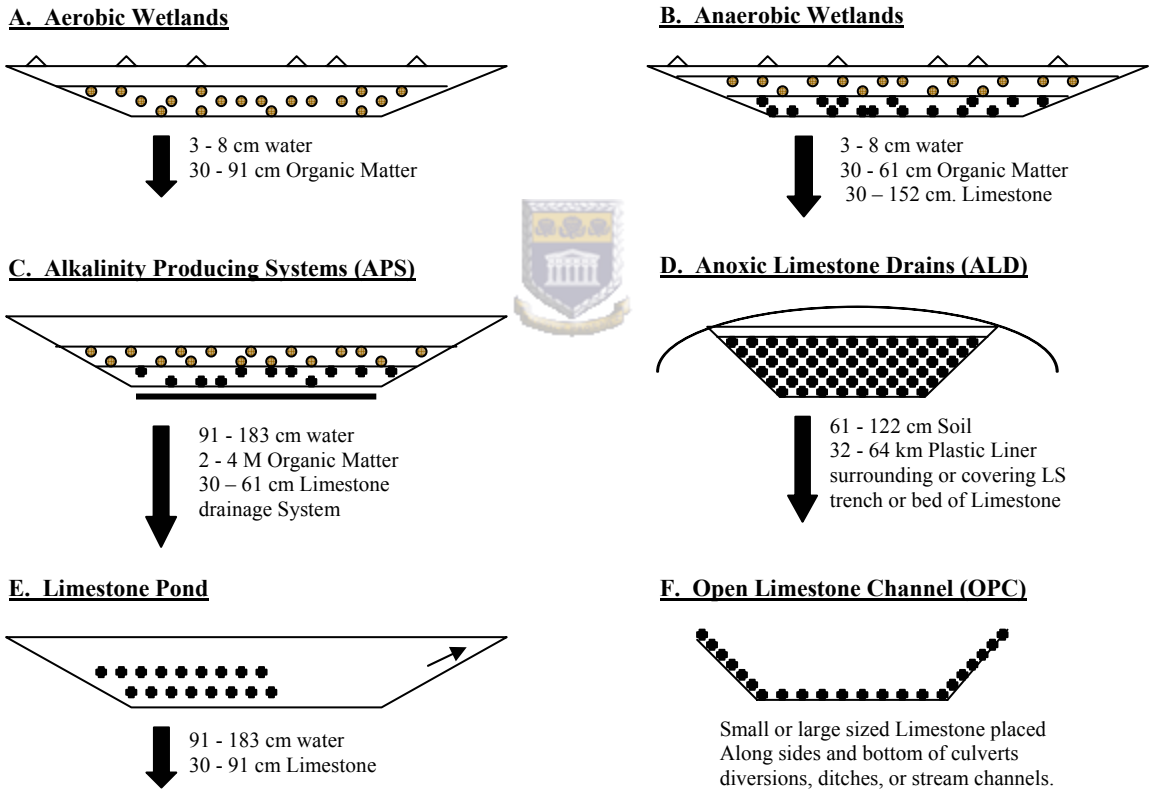

Figure 1.6. Schematic diagram of passive systems for treatment of AMD (Skousen, 1997).

Wetlands

Two types of construction styles are typically used for passive treatment of AMD. Aerobic wetlands consist of *Typha* spp. and other wetland vegetation planted in shallow (< 30 cm) impermeable sediments comprised of soil, clay or mine spoil (Fig. 1.6A). Aerobic wetlands (Fig. 1.6A) collect and aerate water flowing among the planted vegetation, facilitating metal precipitation. However, while iron precipitates, there is typically little effect on aluminium and manganese concentrations (Skousen, 1997; Jage *et al*., 2001).

Anaerobic wetlands consist of *Typha* spp. planted into deep (> 30 cm) permeable sediments (soil, sawdust, straw/manure, or other organic mixtures) which is often high in calcium (Fig. 1.6B) (Jage *et al*., 2001). Anaerobic wetlands promote water flow through organic rich substrates. The limestone layer is usually at the bottom of the wetland or may be mixed with the organic matter (Skousen, 1997). These systems remove significant quantities of iron, but do not significantly adjust the pH due to the slow mixing of acidic surface water with the alkaline substrates (Jage *et al*., 2001).

Alkalinity Producing Systems

The APS (Fig. 1.6C) operate in a similar manner to the anaerobic wetlands, but require a reduced land area. APS are constructed with a layer of composted organic matter on top of a bed of limestone. A layer of AMD water settles on top of the organic layer, and drains into perforated drainage pipes, placed in the lower part of the limestone layer. The water then flows through the organic layer and limestone and is then discharged into an

adjacent settling pond. In the upper portion of the organic layer, dissolved O_2 is removed from the AMD by microbial activity. In the limestone layer Fe^{3+} is reduced to Fe^{2+} because of anaerobic conditions. The limestone then gets dissolved by the anaerobic water with the production of hydroxide ions. Once the water is drawn into the drainage pipes and is discharged into the adjacent settling pond, re-oxygenation of the water and precipitation of the metals occurs (Jage *et al*., 2001).

Anoxic Limestone Drains

The ALD system (Fig. 1.6D) is used to pre-treat AMD. It consists of a trench filled with limestone, covered to exclude O_2, into which anaerobic water is introduced (Jage *et al*., 2001; Skousen, 1997). When AMD water flows through, limestone is dissolved and alkaline bicarbonate is produced. The effluent is then discharged into another treatment system or settling pond to allow for further treatment (acid neutralization, pH adjustment and metal precipitation (Jage *et al*., 2001)).

Limestone Ponds

In Limestone Ponds (Fig. 1.6E), limestone is placed at the bottom of the pond and water flows upward through the limestone. As few limestone ponds have been constructed, little information is available on this treatment (Skousen, 1997).

Open Limestone Channels

The OPC systems (Fig. 1.6F) are open channels or ditches lined with limestone, through which AMD water can be passed directly. This system is an effective mechanism for removing iron (Skousen, 1997).

1.5.2. FA Treatment

FA, which is produced during coal combustion, has a number of possible applications (see Table 1.3).

Table 1.3. Potential uses of municipal solid waste FA (Ferreira *et al*., 2002)

A. Construction Materials	Cement production
	Concrete
	Ceramics
	Glass and glass-ceramics
B. Geotechnical	Road pavement
	Embankment
C. Agriculture	Soil amendment
D. Miscellaneous	Sorbent
	Solid phase conditioning

FA is highly alkaline due to the presence of lime. Several studies have shown that FA can be utilized to neutralize AMD (Gitari *et al*., 2003; Petrik *et al*., 2003; Surender and Petrik, 2005). The treatment of AMD with FA is much more effective than treatment with

lime or limestone. During FA treatment, removal rates of sulfate, Fe, Al and heavy metals are relatively high (Petrik *et al*., 2003).

Because of the removal of potentially toxic metal ions and soluble sulfate, the co-disposal of AMD with FA allows water purification without the addition of expensive chemicals or the usage of high cost passive treatment technologies.

1.5.3. FA-AMD Co-disposal

A co-disposal remediation system, which involves FA and AMD, is currently under development by Eskom for wastewater and effluent treatment. The advantage of this technology is that it involves the co-disposal and detoxification of two recalcitrant and toxic waste products. During the FA-AMD co-disposal process there are potential benefits in the generation of low sulfate, low heavy metal and neutral water streams. The operational format of this continuous FA-AMD co-disposal process is shown in Fig. 1.7.

The AMD input streams [1] contain products, which are highly acidic, while the FA input streams are highly alkaline. The well-characterized mesoacidophilic microbiology of AMD [1] is expected to be inactivated on contact with the highly alkaline FA [2]. The time for mixing the two input phases [3] is relatively short. It is ideally expected that the output phase [4 and 5] should have a sufficiently low biological oxygen demand and toxic chemical load to be returned to the environment. The precipitated solid phase [4] is settled and might be used for landfilling.

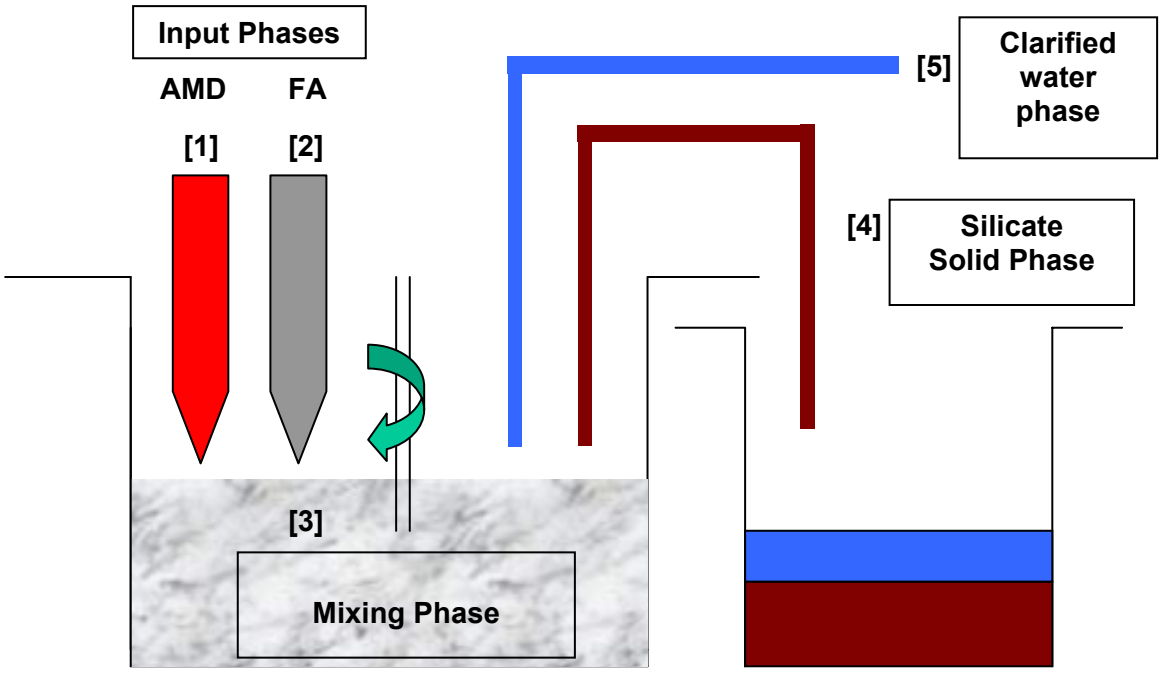

Figure 1.7. Co-disposal of FA and AMD. This system contains five discrete physical phases: AMD [1] and FA [2] input phases; a FA-AMD mixing phase [3]; a precipitated Ca/Fe-SO_4- silicate solid phase [4] and a clarified effluent water phase [5].

Various chemical analyses were done on the co-disposal of FA and AMD (Gitari *et al*., 2003). This includes studies of the major elements and trace elements found in both FA and AMD. This study mainly focuses on the microbial diversity associated with this FA-AMD co-disposal.

1.6. OBJECTIVES OF THE PROJECT

Primary Objective:

The main objective of the work presented in this thesis involves an analysis of the microbial populations associated with the FA-AMD remediation system in order to analyse the microbial impact on this system.

Secondary Objectives:

- Identifying the microbial diversity associated with the input and output phases of the FA-AMD remediation system.
- Determining the survival of microorganisms contributed by the input phases of FA-AMD remediation system.

Questions:

This project was designed to answer the following questions:

- Can microorganisms survive in the input phases of the FA-AMD remediation system?
- Does the co-disposal remediation process influence the microbial diversity associated with the input and output phases?

Chapter 2
Materials and Methods

2.1. MICROBIAL DIVERSITY ASSOCIATED WITH THE INPUT PHASE OF THE FA-AMD REMEDIATION SYSTEM

2.1.1. Sampling

Fly Ash

FA was collected at the Arnot Eskom coal-fired power station near Witbank, Mpumalanga, South Africa. Fresh FA samples were taken directly from the electrostatic precipitator at the power station. The FA samples were collected in airtight bags and sealed tightly to exclude air. Samples were transported to Eskom-Resources and Strategy Division, Johannesburg, South Africa.

Acid Mine Drainage

AMD liquid was collected from an acidic stream flowing from the Landau Colliery near Witbank, Mpumalanga, South Africa. Fresh AMD samples were collected in high-density polyethylene bottles. The bottles were filled and sealed to exclude air. The AMD samples were transported to Eskom-Resources and Strategy Division, Johannesburg, South Africa and stored at 4°C.

The electrical conductivity (EC), pH, total dissolved solids (TDS) and temperature of the AMD samples were monitored before co-disposal, using a portable Hanna pH/EC/TDS/Temperature meter.

2.1.2. Genomic DNA Extraction

Fly Ash

DNA was extracted directly from 0.5 g FA samples using the Fast DNA® Spin Kit for soil (Qbiogene), following the protocol of the manufacturer. Samples were visualized on 0.8% w/v agarose gels as described in section 2.1.3.

Acid Mine Drainage

Metagenomic DNA was extracted directly from AMD liquid samples, using the extraction procedure of Simmons and Norris (2002). Cells were collected from 4 ml samples by centrifugation, and mixed with an extraction buffer, Buffer S, containing 100 mM Tris-Cl (pH 8); 100 mM EDTA (pH 8); 1.5 M NaCl; 1% CTAB. The cells were exposed to a freeze/thaw cycle and treated with 10 µg/µl proteinase K and 20% SDS. After mixing the homogenate with phenol:chloroform:isoamyl alcohol (25:24:1), samples were centrifuged at 12 000 rpm for 10 minutes. DNA was precipitated with 0.7 volumes isopropanol and washed with 70% ethanol. DNA pellets were resuspended into 30 µl TE and stored at -20°C. Genomic DNA was purified using a purification kit from Fermentas (Genomic DNA Purification Kit), following the protocol from the manufacturer. The purified DNA samples were visualized on 0.8% (w/v) agarose gels (see section 2.1.3).

2.1.3. Agarose Gel Electrophoresis

Agarose (Bioline) gels were prepared in 0.5 x TBE buffer (Invitrogen) and heated in a microwave oven until dissolved. Gels were cooled and 500 µg/ml ethidium bromide (BDH) was added. The gels were allowed to set for at least 30 minutes at room

temperature before 5 µl samples, mixed with 2 µl Orange G loading buffer, were loaded. Samples were electrophoresed at 80 Volts until the orange loading dye had migrated to the bottom of the gel. DNA bands were visualized with UV light (312 nm), and recorded on Polaroid film.

2.1.4. 16S rDNA Amplification

Purified genomic DNA served as the template for 16S rDNA PCR reactions for the construction of 16S rDNA libraries. Two microliter samples of bulk genomic DNA were added to each PCR reaction. Amplification was performed in an automated thermal cycler (Thermo Hybaid system). The PCR reaction consisted of 1x PCR buffer, 1.5 mM $MgCl_2$, 0.2 mM of each deoxynucleoside triphosphate, 1 µl *Taq* polymerase (Fermentas), and 0.5 µM of each universal 16S rDNA eubacterial primer (E9F; 5'–GAG TTT GAT CCT GGC TCA G-3' (Farelly *et al*., 1995) and U1510R; 5'–GGT TAC CTT GTT ACG ACT T-3' (Reysenbach *et al*., 1995)). PCR conditions were as follows: an initial denaturation step at 94°C for 2 minutes; 30 cycles of 94°C for 1 minute, 50°C for 1 minute, 72°C for 1 minute; and a final extension step at 72°C for 10 minutes. PCR controls included a negative control (1 µl sterile distilled water as template) and a positive control (10 ng of *E. coli* genomic DNA as template). PCR products were visualised on 0.8% w/v agarose gels (see section 2.1.3).

PCR products were purified from the agarose gel using the GFX-PCR DNA and Gel Band Purification Kit (Amersham Biosciences). The concentration of the purified DNA

was determined electrophoretically by comparison with known DNA concentrations of uncut λ phage DNA (3 ng/µl, 10 ng/µl, 15 ng/µl and 30 ng/µl).

2.1.5. Construction of 16S rDNA Library

Purified 16S rDNA amplicons were cloned into the pMOS*Blue* vector using the pMOS*Blue* blunt ended cloning kit (Amersham Pharmacia Biotech). The cloning procedure was performed as per the manufacturer's instructions, with a 1:2.5 ratio of vector and insert. The following equation was used to determine the amount of 16S rDNA insert required.

$$\left(\frac{(Z).50}{2887} x \frac{2.5}{1}\right) = \text{ng of insert}$$

where Z is the size of insert in bp (1500 bp)

2887 is the size of the vector in bp

50 is the concentration of the vector (ng)

Prior to ligation, the purified 16S rDNA PCR amplicon was treated with phosphokinase in order to generate blunt-ends. The phosphokinase reaction contained 1 µl 10x buffer; 0.5 µl 100 mM DTT; 1 µl phosphokinase; and 7.5 µl insert DNA (16S rDNA PCR amplicons). The phosphokinase reaction was incubated at 22°C for 40 minutes, after which phosphokinase was heat inactivated at 75°C for 15 minutes. The reaction mixture was then placed on ice for 2 minutes. For the ligation reaction, 1 µl of pMOS*Blue* vector (50 ng) and 1µl T4 DNA ligase (4 Weiss units) was added to the phosphokinase reaction and incubated at 22°C overnight. One microlitre of the ligation mix was transformed into

MOS*Blue* competent cells (according to kit specifications). A fifth of the transformation mix was spread on Luria Bertani (LB) solid media supplemented with 20 µl 100 mM isopropyl-beta-D-thiogalactopyranoside (IPTG), 35 µl 50 mg/ml 5-bromo-4-chloro-3-indolyl-beta-D-galactopyranoside (X-gal) and 100 µg/ml ampicillin, and incubated at 37°C overnight.

White colonies were selected randomly and screened for the presence of a 1.5 kb insert by colony PCR. Single colonies were first transferred into 40 µl 1x TE and heated at ±99ºC for 3 minutes in a PCR machine (Thermo Hybaid system) to lyse the cells and denature DNAse enzymes. After centrifugation, 20 µl of each supernatant was transferred to a clean eppendorf tube for M13 PCR amplification. The PCR reaction consisted of 1x PCR buffer, 1.5 mM $MgCl_2$, 0.2 mM of each deoxynucleoside triphosphate, 1 µl *Taq* polymerase (Fermentas), and 0.5 µM of each of the vector derived PCR primers (pUCM13F; 5'–GTT TTC CCA GTC ACG AC-3' and pUCM13R; 5'–CAG GAA ACA GCT ATG AC-3'). Each reaction was adjusted to a final volume of 50 µl with sterile distilled water and amplified in an automated thermal cycler (Thermo Hybaid system). PCR conditions were as follows: an initial denaturation step at 94^{o}C for 5 minutes; 30 cycles of 94^{o}C for 30 seconds, 65^{o}C for 45 seconds, 72ºC for 1 minute; and a final extension step at 72^{o}C for 10 minutes. PCR controls included a negative control (5 µl sterile distilled water as template). PCR products were visualized on 1% w/v agarose gels (see section 2.1.3).

2.1.6. Amplified rDNA Restriction Analysis (ARDRA)

Clones shown to contain plasmids with 1.5 kb inserts were selected for Amplified rDNA Restriction Analysis (ARDRA) (Martin-Laurent *et al*., 2001). Two different restriction enzymes, *Mbo*I (4 bp cutter; Fermentas) and *Rsa*I (4 bp cutter; Fermentas), were used to digest the 1.5 kb 16S rRNA gene PCR amplicons to produce restriction enzyme patterns. The digestion reactions contained 5.0 µl PCR reaction mix, 1 U restriction enzyme, 1.5 µl 10x buffer and 8.4 µl distilled water. Restriction enzyme digestions were incubated at 37°C overnight. The *Mbo*I and the *Rsa*I digestion products were visualized on 2.5% w/v agarose gels as described in section 2.1.3. The restriction profiles were compared to identify clones with a unique restriction pattern.

2.1.7. Sequencing and BLAST Analyses

Twenty-nine clones were sequenced by Inqaba Biotech (Johannesburg, SA) using the M13F (5` - CGC CAG GGT TTT CCC AGT CAC GAC - 3`) and M13R (5` - GAG CGG ATA ACA ATT TCA CAC ACA AGG - 3`) primers. The sequences of each of the clones were analysed using software packages, BioEdit Version 7.0 (Hall, 1999) and DNAMAN Version 4.13. The GenBank database was searched for similar sequences using BLAST software (Altschul *et al*., 1997). Sequences from the clones and data base were aligned using ClustalX (Thompson *et al*., 1997) and the software package Phylo_win Version 2.0 (Galtier *et al*., 1996) was used for the construction of phylogenetic trees based on maximum-parsimony analysis.

2.2. MICROBIAL DIVERSITY ASSOCIATED WITH THE CO-DISPOSAL SAMPLES

2.2.1. Co-disposal Experiments

Co-disposal (mixing) experiments were undertaken at Eskom-Resources and Strategy Division (Rosherville, Johannesburg) by Ms. Damini Surender, using a pilot scale mixer consisted of a turbulator/aerator mixing unit with a 250 L capacity. The unit was designed with a conical base, which allowed separation of the solid phase from the liquid (shown in Fig. 2.1).

A ratio of 1:6 FA:AMD was used for all co-disposal experiments. Approximately 200 L of fresh AMD was added to mixing unit with approximately 30 kg of fresh FA, and stirred at approximately 1500 rpm. A top view of the tank in Fig. 2.2 shows the mixing of the AMD and FA.

During the 2 hour mixing period samples were collected at specified time intervals (t = 2min, 4min, 6min, 20min, 30min, 45min, 60min, 100min and 120min). All co-disposal samples were kept at 4^{o}C during transportation and stored at -20^{o}C.

Figure 2.1. The pilot scale mixer and turbulator/aeration unit.

Figure 2.2. A top view of the pilot rig, showing the stirring of FA and AMD.

2.2.2. pH Analyses

The pH of each sample was monitored at the point of collection with a portable Hanna pH/EC/TDS/Temp. meter.

2.2.3. Genomic DNA Extraction

Metagenomic DNA was extracted directly from the co-disposal samples using the extraction procedure outlined by Simmons and Norris (2002) (see section 2.1.2).

To test whether the chemical composition of FA inhibited DNA extraction from the co-disposal samples, *E. coli* was inoculated into the co-disposal liquid prior to extraction of DNA. Extracted DNA was visualised on 1% w/v agarose gels (see section 2.1.3).

2.3. SURVIVAL OF MICROORGANISMS FROM THE INPUT PHASE DURING CO-DISPOSAL

2.3.1. Culture Media

The survival of AMD-derived microorganisms during the co-disposal process was assessed by determining the culturability of *At. ferrooxidans* on a medium specific for this organism. *At. ferrooxidans* medium contained the following mineral salts (in grams per liter): $(NH_4)_2SO_4$, 2.0; KCl, 0.1; K_2HPO_4, 0.5; $MgSO_4 \cdot 7H_2O$, 0.5 and $Ca(NO_3)_2$, 0.01; dissolved into 700ml distilled water (Duquesne *et al.*, 2003). The media also contained 40 g/l ferrous sulphate and 2.0 ml/l 1N H_2SO_4, dissolved into 300 ml distilled water. The pH of both solutions (mineral salts and ferrous sulphate solution) was adjusted to pH 1.8 – 2.0 with a pH 4.0 buffer solution. The mineral salts solution was heat sterilized at 121°C

for 15 minutes, while the ferrous solution was filter sterilized by passage through 0.2 µm membrane filters (Kimix). The mineral salts and ferrous sulphate solutions were mixed prior to dispensing.

2.3.2. Culturing of *At. ferrooxidans*

To test the presence of *At. ferrooxidans* in AMD, 1ml of AMD liquid was transferred into 9 ml of sterile culture medium. The control tube was not inoculated. Enriched cultures and the control tube were incubated for up to 4 weeks at ±23°C. A similar protocol was used, to test the survival of *At. ferrooxidans* in co-disposal samples.

2.4. MICROBIAL DIVERSITY ASSOCIATED WITH THE MATURING SETTLED SOLID PHASE (OUTPUT PHASE)

2.4.1. Preparation of pot trials

Pot trials were designed to evaluate the microbial diversity associated with the maturing settled solid phase. The solid phase was aseptically transferred into three pots (A – C). Pot dimensions were: height, 25 cm; diameter, 20 cm; volume approximately 7 L. Pot A containing 100 % solid phase was aerobic; pot B containing 100 % solid phase was anaerobic; pot C containing 50 % moist garden soil and 50 % solid phase was aerobic (shown in Fig. 2.3).

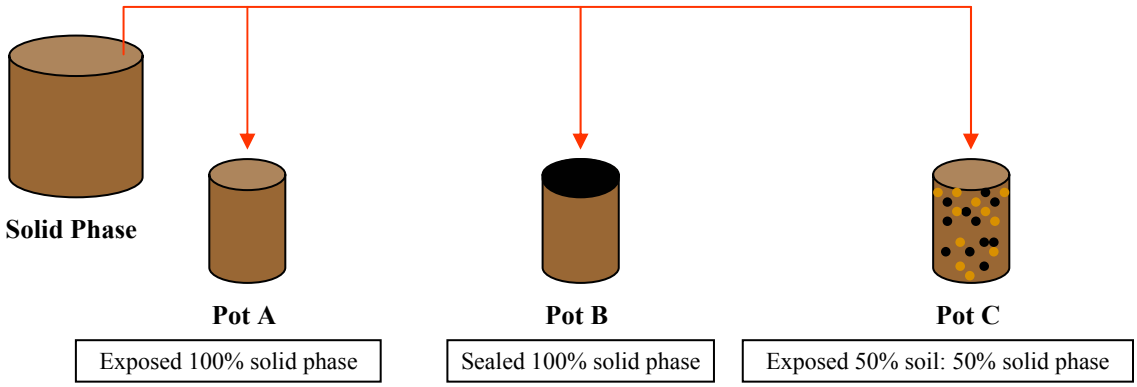

Figure 2.3. A diagram of the pot trials.

Samples from each pot were taken in triplicate (using a 1 cm diameter corer) at bi-weekly intervals for 10 weeks. All pot trial samples were stored at -20ºC until required for future analyses.

2.4.2. Genomic DNA Extraction

Extraction of DNA from solid phase samples was performed using the FastDNA® Spin Kit for soil (Qbiogene), following the protocol of the manufacturer. Extracted DNA was purified using self constructed polyvinylpolypyrrolidone (PVPP) (Berthelet *et al*., 1996) and Sephacryl minicolumns. DNA was visualized on 1% w/v agarose gels (see section 2.1.3). The DNA concentrations of the samples were measured using a Nanodrop ND-1000. Where DNA could not be recovered seeding experiments were done with a test organism (*E. coli*) to assess extraction efficiency. A dilution series (10^3 – 10^{11}) of *E. coli* cells was prepared and 1 ml of each dilution was mixed with 1 g of the sterile solid phase prior to DNA extraction. DNA was then extracted from both the *E. coli* cell dilutions and the seeded solid phase samples.

Chapter 3
Results and Discussion

3.1. INTRODUCTION

In order to further understand the role of microbial processes in the Fly Ash-Acid Mine Drainage (FA-AMD) remediation system, the following were evaluated: the input phases (FA and AMD), the co-disposal samples, the possible survival of microbial cells from the AMD input phase in co-disposal samples, and the output phase.

The total microbial diversity of FA and AMD was determined using well-established molecular phylogenetic methods. Co-disposal experiments using FA and AMD were performed in a pilot scale mixer consisting of a turbulator/aerator unit. Co-disposal samples were taken at different time intervals over a 2 hour period, and used for genomic DNA extractions. For testing the survival of microorganisms contributed by AMD, *At. ferrooxidans* was used as a model organism. Culture media specific for *At. ferrooxidans* were used. Subsequently, attempts were made to culture *At. ferrooxidans* from the co-disposal samples. The output phases of the FA-AMD co-disposal system consisted of the liquid phase (supernatant) and the precipitated solid phase. Ideally, the precipitated solid phase should be chemically and physically stable, such that it could be safely used for landfilling, agricultural soil remediation or other back-filling processes. However, if the development of microbial communities in the maturing solid phase occurs, it might create a source of chemical instability (e.g., via methanogenesis, sulfidogenesis or redox-dependent mineral mobilization). The solid phase was tested for development of microbial communities with three pot trials using co-disposed FA-AMD solid phase.

3.2. MICROBIAL DIVERSITY ASSOCIATED WITH THE INPUT PHASE OF THE FA-AMD REMEDIATION SYSTEM

3.2.1. Characteristics of AMD

Characteristic values were measured for the AMD input phase (shown in Table 3.1).

Table 3.1. Characteristic measurements of the AMD.

Measurement	Value
pH	2.68
Electrical Conductivity (EC)	14.19 ms/cm
Total Dissolved Solids (TDS)	7008 mg/L
Temperature	23°C

The results obtained from the AMD before the co-disposal process show that AMD is highly acidic. This low pH is an indication of a deficiency of calcareous minerals and the absence of carbonate buffering in the AMD sample (Gitari *et al*., 2003). The low pH is also indicative that acidophilic microbial populations could be present. The EC is relatively high compared to that of other AMD sites (average 10 – 11 ms/cm). The measurement for TDS is ~ 30% higher than previous studies have determined (average 4000 – 5000 mg/L) (Gitari *et al*., 2003).

3.2.2. Genomic DNA Extraction

Fly Ash

Attempts to extract DNA from FA samples were unsuccessful. This was consistent with expectations, given the high temperature origins of the FA samples (approximately 1000ºC) (data not shown).

Acid Mine Drainage

Metagenomic DNA extracted from AMD liquid samples yielded low concentrations of DNA. Yields were sufficiently low that the extracted metagenomic DNA was not visible on agarose gels (data not shown).

3.2.3. 16S rDNA Amplification

PCR amplification of eubacterial 16S rDNA genes from the AMD sample yielded a 1.5 kb fragment (see lane 1 in Fig. 3.1). Other amplifications of AMD-derived DNA sample were not successful, yielding only primer-dimers (lane 3). The PCR product in lane 1 was used for the construction of a 16S rDNA library.

The concentration of the DNA extracted from the AMD was approximately 25 ng/µl as determined electrophoretically by comparison with known DNA concentrations of uncut λ phage DNA (see Chapter 2, section 2.1.4; data not shown).

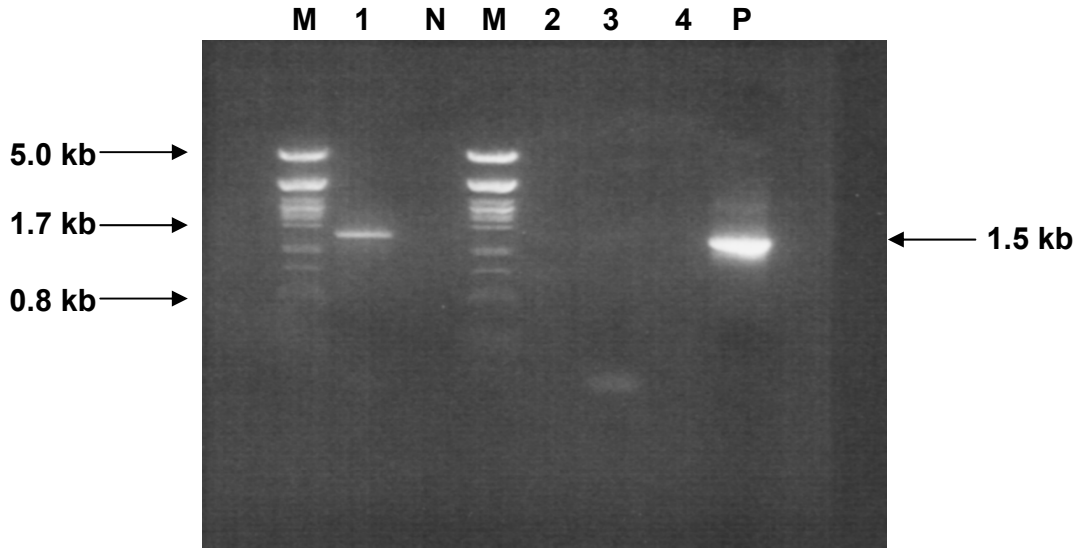

Figure 3.1. PCR amplification of bulk genomic DNA (lane 1 and 3). PCR products were separated by size on a 0.8% w/v agarose gel. M depicts the DNA molecular weight marker (λ DNA restricted with *Pst*I); N is the negative control; and P is the positive control (*E. coli*).

3.2.4. Construction of 16S rDNA Library

A 16S rDNA library was constructed by cloning the 1.5 kb 16S rDNA amplicons into the pMOS*Blue* vector (Amersham Pharmacia Biotech). Transformation results indicated that approximately 65% of the library contained recombinant clones, appearing as white colonies. The remaining 35% of the library consisted of blue colonies, indicating religated vector (shown in Table 3.2).

Table 3.2. Transformation results.

LB solid media + Amp + IPTG + X-Gal	**Nr. of blue colonies**	**Nr. of white colonies**
AMD sample	43	81
Positive control	TNTC*	0
Negative control	0	0

*TNTC: To numerous to count

The 81 white colonies were randomly chosen for direct colony PCR (pMOS*Blue* blunt ended cloning kit, Amersham Pharmacia Biotech), using vector-derived primers (shown in Fig. 3.2).

Forty out of 81 white colonies contained a 1.5 kb insert (Figure 3.2). The remaining 41 white colonies either contained recombinant plasmids with an insert smaller than 1.5 kb (e.g. lanes 6, 10, 19) or contained only the vector (e.g. lanes 7, 20), (i.e., they were false positive clones; Figure 3.2).

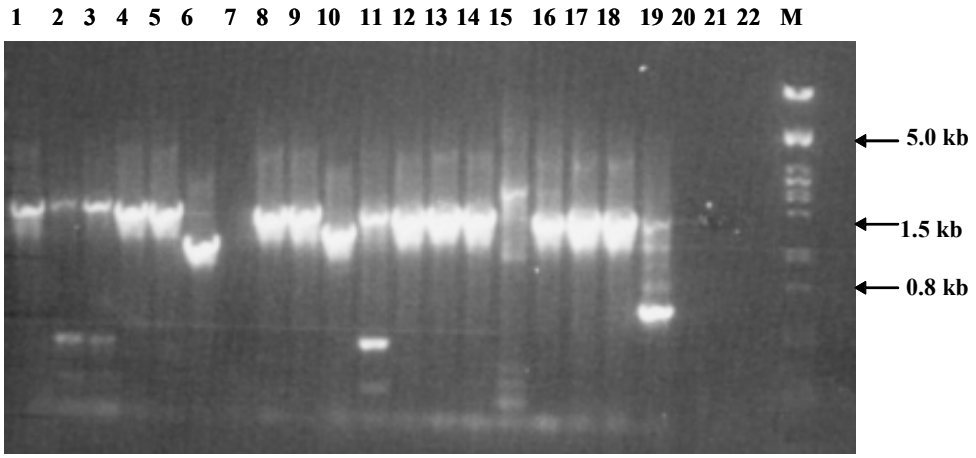

Figure 3.2. Colony PCR amplicons of some of the 81 randomly chosen white colonies. PCR products were separated on 1% w/v agarose gels. M depicts the DNA molecular weight marker (λ DNA restricted with *Pst*I).

3.2.5. Amplified rDNA Restriction Analysis (ARDRA)

The forty positive colony PCR amplicons were analysed further by ARDRA. Fig. 3.3a shows the different restriction patterns of the PCR amplicons obtained after *Mbo*I digestion. Some of the amplified 16S rDNA PCR products show identical restriction profiles (e.g. lane 3, 6 and 8; lane 5 and 11). All the other fragments have a unique restriction profile.

Fig. 3.3b shows the different restriction patterns of the PCR amplicons obtained after *Rsa*I digestion. PCR amplicons in lanes 2 and 8 have similar restriction patterns, while lanes 11 and 20 contain amplicons with similar restriction patterns. The rest of the amplicons shown in Fig. 3.3b have unique restriction patterns.

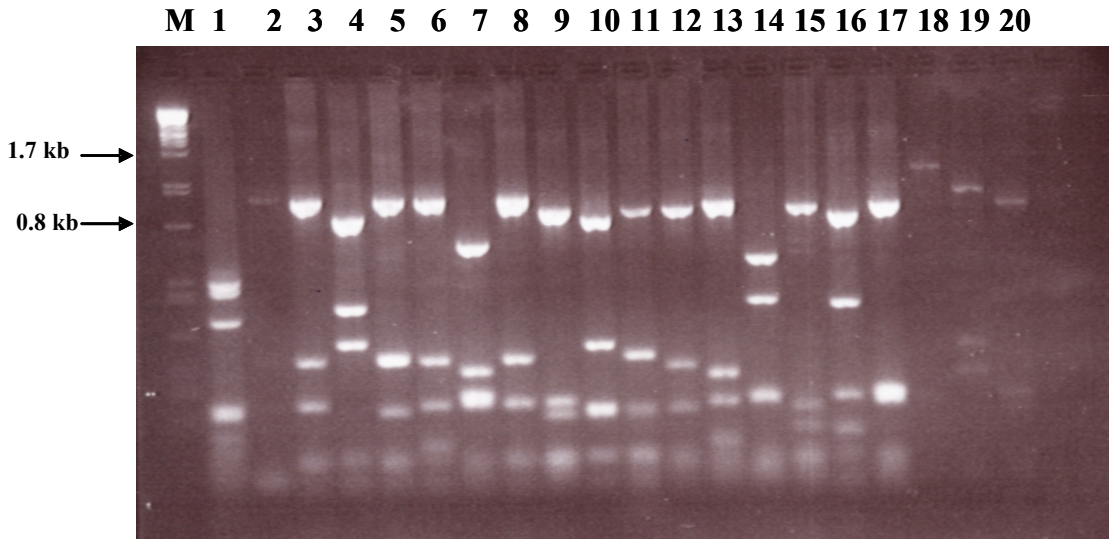

Figure 3.3a. ARDRA of some of the positive colony PCR amplicons shown on a 2.5% w/v agarose gel. *Mbo*I restriction enzyme digestion of colony PCR amplicons. M depicts the DNA molecular weight marker (λ DNA restricted with *Pst*I); and lanes 1 – 20 represents the colony PCR amplicons.

After restriction enzyme digestion with both *Mbo*I and *Rsa*I, a wide variety of different restriction patterns were obtained. The patterns for each clone were compared and the results indicated that there were 29 unique types. Representative clones from each group were sent to Inqaba Biotech (Johannesburg, SA) for sequencing.

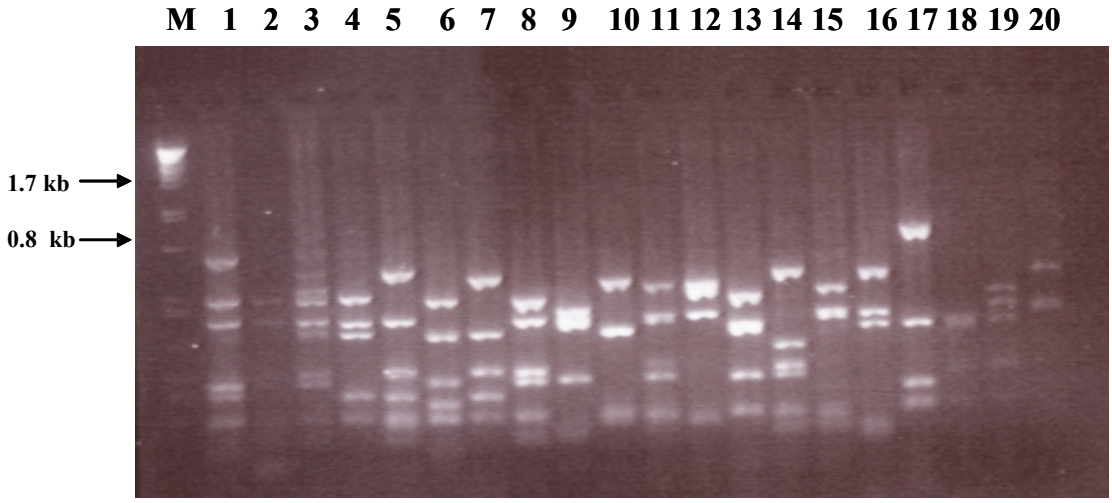

Figure 3.3b. ARDRA of some of the positive colony PCR amplicons shown on a 2.5% w/v agarose gel. *Rsa*I restriction enzyme digestion of colony PCR amplicons. M depicts the DNA molecular weight marker (λ DNA restricted with *Pst*I); and lanes 1 – 20 represents the colony PCR amplicons.

3.2.6. Sequencing and BLAST Analyses

Sequencing results of the clones were compared to similar sequences in the GenBank database using BLAST software (Altschul *et al*., 1997). Putative identification data based on sequence similarity are shown in Table 3.3.

16S rDNA sequences were aligned with sequences in GenBank using ClustalX (Thompson *et al*., 1997) and a maximum parsimony phylogenetic tree (shown in Fig. 3.4) was constructed with the software package Phylo_win Version 2.0 (Galtier *et al*., 1996). *Escherichia coli* (marked with blue box) was used to root the tree. The clones are labeled pAMD (in black) and the strains from GenBank are shown in red.

Table 3.3. Results of BLAST analysis of 29 clones.

AMD Clone	Length (bp)	% Similarity	Accession Number	Organism	Reference
pAMD 2	679	99%	AF353297	Uncultured bacterium Tui3-12	Unpublished
pAMD 9	788	97%	AF353297	Uncultured bacterium Tui3-12	Unpublished
pAMD 13	785	91%	AF356834	*Leptospirillum ferrooxidans*	Coram and Rawlings, 2002
pAMD 17	300	98%	AF353297	Uncultured bacterium Tui3-12	Unpublished
pAMD 20	784	98%	AF460989	Uncultured *Thiomonas* sp. C19	Battaglia-Brunet *et al.*, 2002
pAMD 23	774	99%	AJ278723	*Acidithiobacillus ferrooxidans*	Selenska-Pobell *et al.*, 2001
pAMD 24	777	99%	AF460989	Uncultured *Thiomonas* sp. C19	Battaglia-Brunet *et al.*, 2002
pAMD 27	785	99%	D30775	*Acidiphilium organovorum*	Kishimoto *et al.*, 1995
pAMD 30	534	99%	AY65999	Acid streamer iron-oxidizing bacterium	Unpublished
pAMD 31	781	99%	AF376026	*Acidiphilium* sp. NO-17	Unpublished
pAMD 36	777	98%	AF376020	*Acidithiobacillus sp.* NO-37	Johnson *et al.*, 2001
pAMD 37	783	93%	AJ278723	*Acidithiobacillus ferrooxidans*	Selenska-Pobell *et al.*, 2001
pAMD 39	575	98%	AF356834	*Leptospirillum ferrooxidans*	Coram and Rawlings, 2002
pAMD 41	686	100%	AY65999	Acid streamer iron-oxidizing bacterium	Unpublished
pAMD 43	690	100%	D30773	*Acidiphilium cryptum*	Kishimoto *et al.*, 1995
pAMD 45	433	89%	AF225451	Uncultured bacterium BA84	Bond *et al.*, 2000
pAMD 46	788	99%	AF356839	*Leptospirillum ferrooxidans* strain Sy	Coram and Rawlings, 2002
pAMD 48	731	99%	AB023643	*Acidiphilium* sp. MBIC4287	Unpublished
pAMD 49	581	97%	AF460989	Uncultured *Thiomonas* sp. C19	Battaglia-Brunet *et al.*, 2002
pAMD 51	607	98%	D30773	*Acidiphilium cryptum*	Kishimoto *et al.*, 1995
pAMD 54	756	99%	AF353297	Uncultured bacterium Tui3-12	Unpublished
pAMD 55	643	99%	AB006711	*Acidiphilium multivorum* strain: AIU 301	Unpublished
pAMD 56	698	99%	AF356839	*Leptospirillum ferrooxidans* strain Sy	Coram and Rawlings, 2002
pAMD 57	787	96%	AF460989	Uncultured *Thiomonas* sp. C19	Battaglia-Brunet *et al.*, 2002
pAMD 58	760	99%	AF353297	Uncultured bacterium Tui3-12	Unpublished
pAMD 60	578	100%	AF356839	*Leptospirillum ferrooxidans* strain Sy	Coram and Rawlings, 2002
pAMD 62	617	99%	AY632901	*Acidiphilium symbioticum*	Unpublished
pAMD 67	507	99%	AF353297	Uncultured bacterium Tui3-12	Unpublished
pAMD 76	713	100%	AF353297	Uncultured bacterium Tui3-12	Unpublished

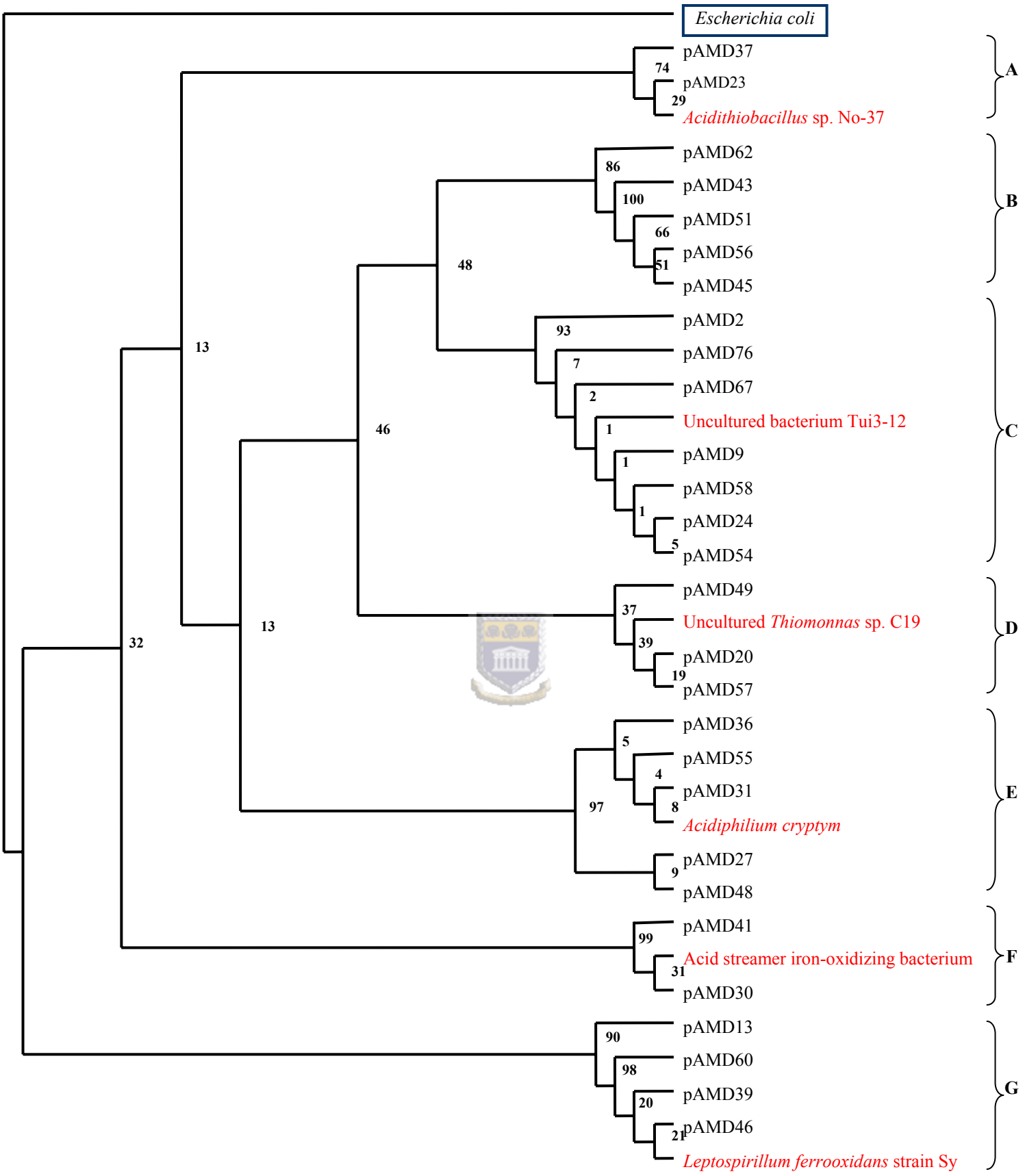

Figure 3.4. Phylogenetic tree based on maximum-parsimony analysis (1000 bootstraps).

The results of BLAST and phylogenetic analyses (shown in Table 3.3 and Fig. 3.4) confirmed the presence of organisms with a high sequence similarity to known acidophiles in the AMD. Table 3.3 shows that 55% of the 29 clones had the highest degree of similarity with uncultured bacteria found in acidic environments, while the other 45% showed sequence similarity with *Acidithiobacillus* spp., *Acidiphilium* spp., and *Leptospirillum* spp. *Leptospirillum ferrooxidans* and *Acidiphilium cryptum* were the most commonly identified species. All these organisms are commonly identified in acidophilic habitats (Baker and Banfield, 2003).

pAMD 17 was excluded from the phylogenetic tree as the recovered sequence was too short (300 bp). Fig. 3.4 shows that all the AMD clones grouped into six groups (A - F). Group A (pAMD 37 and 23) are related to *Acidithiobacillus* spp., belonging to the γ-proteobacteria. Group B does not cluster with any of the GenBank strains, but is related to group C, which shows similarity to uncultured bacteria found in acidic environments. Group E (pAMD 36, 55, 31, 27 and 48) is related to *Acidiphilium* spp. which belongs to the α-proteobacteria division, and group F (pAMD 41 and 30) are closely related to an acid streamer iron-oxidizing bacterium, which belongs to the actinobacteria. Group G (pAMD 13, 60, 39 and 46) is related to *Leptospirillum ferrooxidans*, which belongs to the nitrospira division.

Phylogenetic analyses of AMD successfully identified a range of typical acidophilic bacterial phylotypes. It is therefore concluded that these organisms will be present at the

beginning of the FA-AMD mixing phase, and are the major contribution to the input biomass.

3.3. MICROBIAL DIVERSITY ASSOCIATED WITH THE CO-DISPOSAL SAMPLES

3.3.1. pH Analyses

Periodic pH analyses indicated that the initial pH of the AMD liquid was 2.68, but increased rapidly on contact with the Fly Ash; i.e., the pH increased to 6.03 within the first two minutes of mixing (shown in Fig. 3.5). After the first two minutes, subsequent pH increases were slow, with an apparent equilibrium pH of 6.3 being reached within 20 minutes.

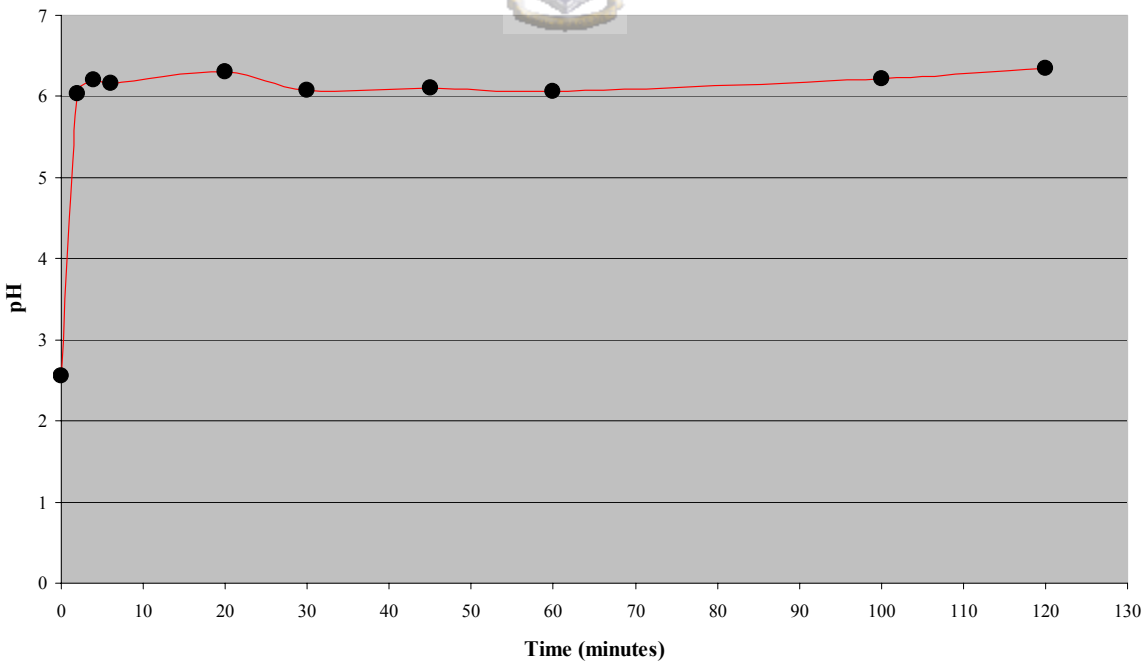

Figure 3.5. pH values of samples recovered during the co-disposal mixing phase.

3.3.2. Genomic DNA Extraction

DNA could not be extracted from the co-disposal samples (data not shown). The reason for this could be the drastic increase in pH (see section 3.3.1). The high pH of the FA is expected to have negative effects on the bacteria present in the AMD input phase. It is likely that as a result of this change in the environmental pH, acidophile cells are lysed, releasing DNA and cellular contents into the FA-AMD sample. It is suggested that DNA is rapidly degraded (e.g., by exogenous nucleases or chemical breakdown) leading to the subsequent failure to isolate detectible yields of DNA.

To confirm whether the failure to extract DNA was not the result of a chemical interaction between the cells and the FA, a series of seeded extraction trials were performed (shown in Fig. 3.6). A visible band in lane 1 (Fig. 3.6) indicated that *E. coli* genomic DNA was successfully extracted from the co-disposal solid phase sample. The absence of a visible band in lane 2 (Fig. 3.6), indicates that detectable DNA could not be extracted from the co-disposal water (supernatant phase). These results suggest that the chemical composition of FA does not inhibit recovery and extraction of DNA from the co-disposal samples.

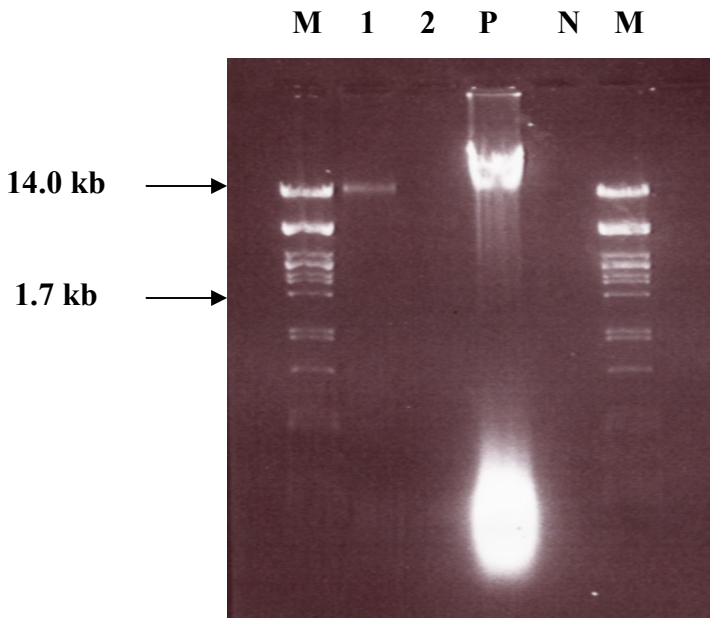

Figure 3.6. Extracted DNA from co-disposal samples on 1% w/v agarose gel. Lane M depicts the molecular weight marker (λ DNA restricted with *Pst*I). Lane 1, co-disposal water inoculated with *E. coli*; lane 2, co-disposal water; lane P, positive control (*E. coli*) and lane N, negative control (sterile water).

3.4. SURVIVAL OF MICROORGANISMS FROM THE INPUT PHASE DURING CO-DISPOSAL

3.4.1. Culturing of *At. ferrooxidans*

To confirm that the bacteria found in AMD liquid did not survive the co-disposal process, culturing of acidophilic organisms from AMD liquid and co-disposal samples was attempted. After an incubation period of four weeks, culture tubes containing the AMD-water (Fig. 3.7a; tube 2) showed a reddish brown precipitate, while the control tube (Fig. 3.7a; tube 1), remained clear. The reddish brown precipitate in test tube 2 is almost certainly due to iron oxidation ($Fe^{2+} \rightarrow Fe^{3+}$; as described in Chapter 1.4.4.2), an

indication that iron reducing bacteria (*At. ferrooxidans*)cells are present. Light microscopy of Gram stained samples showed the presence of gram negative rod-shaped organisms in tube 2, while none were detectible in the control culture.

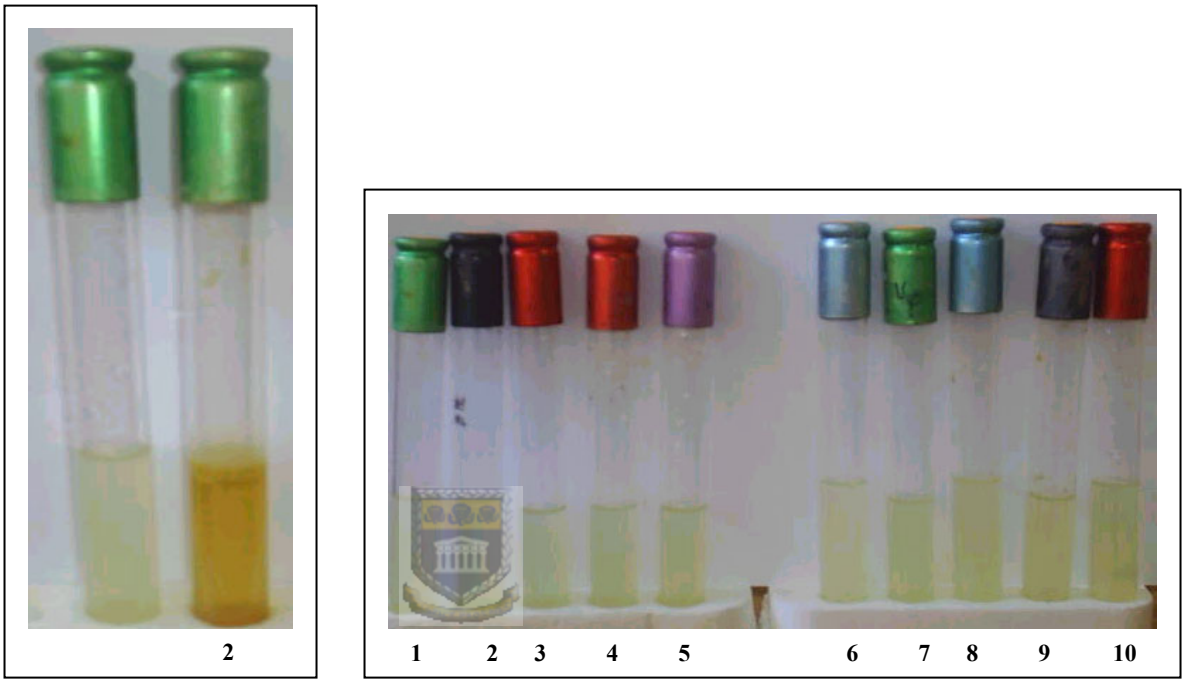

(a) **(b)**

Figure 3.7a-b. Culturing of *At. ferrooxidans* from AMD liquid (a) and co-disposal samples (b).

Attempts to produce viable cultures from co-disposal samples were all negative, even after an incubation period of four weeks. The tubes (Fig. 3.7b; tubes 2-10) showed no color change, and remained indistinguishable from the control (Fig. 3.7b; tube 1). Light microscopy also showed the absence of cells within the co-disposal samples.

These results indicate that *At. ferrooxidans* found in AMD were not viable co-disposal with FA. Even within the first 2 minutes of mixing, cell viability was apparently reduced below culturable limits. This result is not surprising, given the obligate requirement of these organisms for acidophilic conditions.

3.5. MICROBIAL DIVERSITY ASSOCIATED WITH THE MATURING SETTLED SOLID PHASE (OUTPUT PHASE)

3.5.1. Introduction

After the co-disposal of FA and AMD, a precipitated solid phase develops that needs to be disposed of. The microbial communities that mature in the settled solid phase should be investigated to test the chemical and physical stability of the output phase. For the analysis of the development of microbial communities, pot trials were established with different ratios of soil and solid phase (see chapter 2, section 2.4.1).

3.5.2. Genomic DNA Extraction

DNA could not be extracted from pot A, containing the 100 % solid phase (aerobic) (Figure 3.8, lanes 2) and pot B containing 100 % solid phase (anaerobic) (Figure 3.8, lanes 3).

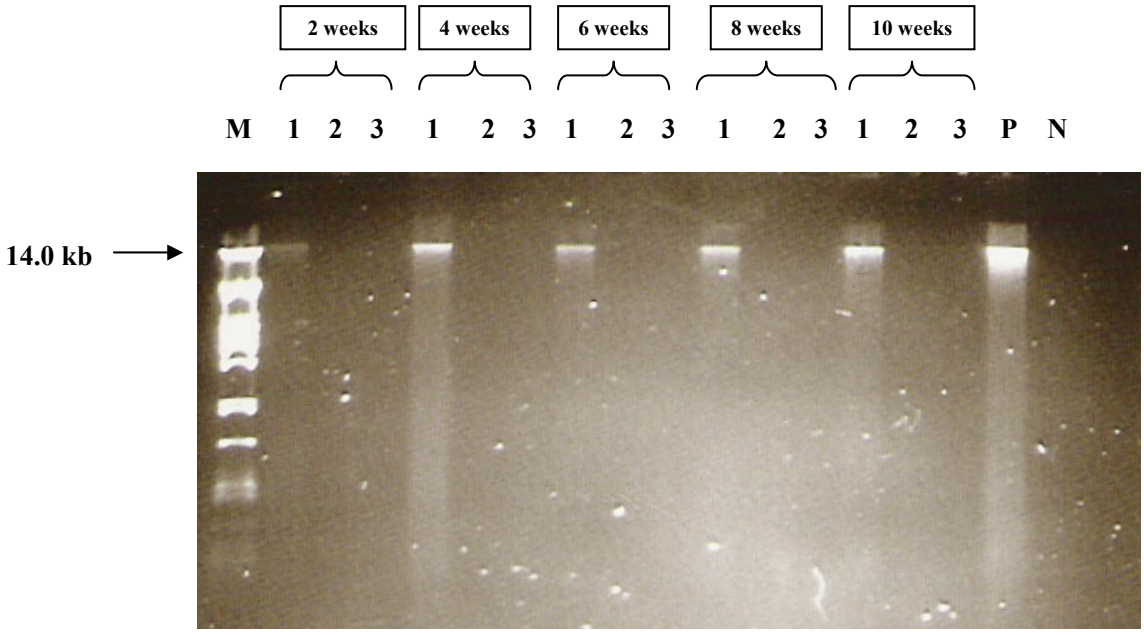

Figure 3.8. Genomic DNA Extraction from the maturing AMD-FA solid phase. Products were separated by size on 1% agarose gels. DNA was investigated after 2-, 4-, 6-, 8-, and 10 weeks. There are three lanes per timepoint with lane 1 pot C, lane 2 pot A and lane 3 pot B. M depicts the DNA molecular weight marker (λ DNA restricted with *Pst*I). Lane P, *E. coli* as a positive control; lane N, negative control.

There is no obvious explanation for the failure to extract DNA from pot A, even after 10 weeks of exposure to atmospheric conditions. Possibly the incubation period was too short, or the presence of toxic elements might have inhibited the development of a microbial community.

It is not surprising that DNA could not be extracted from pot B. The constituents are expected to be essentially sterile. The samples were assembled under sterile conditions, and the pot sample was sealed, thus preventing seeding from the environment.

Seeding trials were carried out on the sterile solid phase samples (pot A and pot B) to confirm that the failure to extract DNA from these samples was not due to DNA degradation or absorption caused by the solid phase. The amount of DNA extracted from the seeded solid phase sample (Fig. 3.9, lane 1) and untreated *E. coli* cells (Fig. 3.9, lane 2) were comparable. After a dilution series of *E. coli* cells ($8 \times 10^{11} - 8 \times 10^{3}$) was seeded into the solid phase. DNA could only be recovered from the samples containing 8×10^{11} and 8×10^{10} cells (Fig. 3.9). The yield of extracted genomic DNA was similar for seeded solid phase and neat *E. coli* cells. This suggests that DNA was not absorbed or broken down. Furthermore the minimum number of cells that is necessary within the solid phase samples for successful genomic DNA extraction should be at least 10^{10} cells.

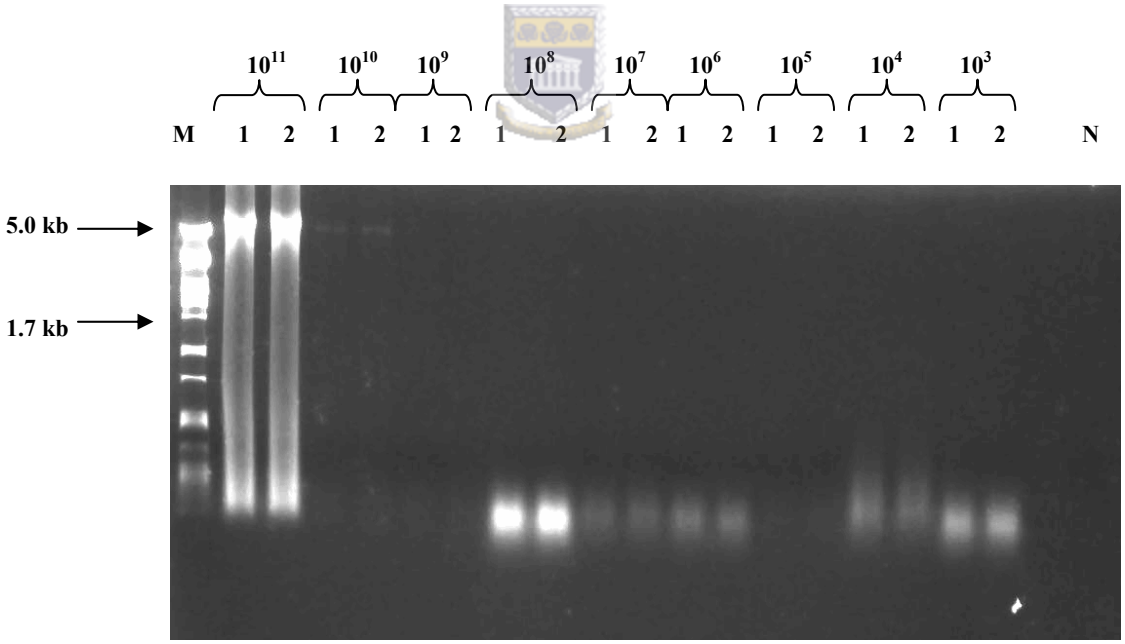

Figure 3.9. Seeding experiment of solid phase sample with *E. coli*. Products were separated by size on 1% agarose gels A dilution series of the *E. coli* cells was prepared ($10^{3} - 10^{11}$). Lane 1 contains the solid phase sample seeded with *E. coli* and lane 2 contains the *E. coli* cells. M depicts the DNA molecular weight marker (λ DNA restricted with *Pst*I); lane N, negative control.

DNA was successfully extracted from samples taken from pot C, containing a 1:1 mixture of moist garden soil and FA-AMD solid phase (Figure 3.8, lanes 1). A low concentration of DNA was extracted. Possible reasons for this are that:

1) The FA-AMD solid phase inhibited DNA extraction (supported by findings that DNA could also not be extracted from pot B).
2) A low number of microbial organisms developed, due to a limited incubation time of the solid phase pot trial samples.

Extensive purification was needed for the genomic DNA extracted from pot C due to the nature of the solid phase. After the first purification step, using PVPP, 16S rDNA amplification of the extracted DNA was not possible. A second purification step, using Sephacryl, was included to remove possible PCR inhibitors. The yield of the DNA after purification was low (1-2 ng/µl) and even after the second purification, amplification was not possible. Therefore the microbial diversity within pot C could not be evaluated. The reasons for this could be the presence of high concentration of PCR inhibitors or excessive loss of DNA during the purification steps.

The results obtained from the solid phase samples indicate that the pots should be incubated for more than two months, allowing time for a microbial community to develop and mature. After microbial development, further analyses could give a better understanding of the chemical and physical stability of the maturing solid phase.

Chapter 4
General Discussion and Conclusion

Disposal of FA and the formation of AMD are of great concern to the coal mining and coal-dependant power generating industries. The neutralization of acidic AMD using alkaline FA has been shown to be effective for the "detoxification" of both materials (Surender and Petrik, 2005).

Previous chemical studies of the FA-AMD co-disposal remediation system have shown that precipitates are formed, which remove a high proportion of heavy metals present in AMD (Gitari *et al*., 2003; Petrik *et al*., 2003; Surender and Petrik, 2005). Sulfate concentrations were reduced and there was a decrease in electrical conductivity (Surender and Petrik, 2005). Aluminium and silicon for zeolite hydrothermal synthesis are also produced (Gitari *et al*., 2003). Other studies show that the solid phase, which is formed during co-disposal, could be used for the large scale production of high capacity ion exchange material with applications for secondary effluent treatment (Petrik *et al*., 2003).

This study investigates the aspects of microbial populations associated with the FA-AMD co-disposal remediation process. The input, co-disposal, and output phases of this system were studied individually. The two input phases, FA and AMD, have a pH of 12.1 and 2.7, respectively. DNA could not be extracted from the FA samples, consistent with the high temperature origins of FA (approximately 1000°C) which presumably render it sterile. Metagenomic DNA extracted from the AMD input phase showed a range of phylotypes typical of acidophilic aquatic environments. The phylotypes included *At.*

ferrooxidans, *Acidiphilium cryptum* and *Leptospirillum ferrooxidans*. During the co-disposal process, pH analysis indicated that after mixing, the pH of the co-disposal samples increased drastically from 2.7 to 6.0 in 2 minutes, which is likely to kill/lyse acidophiles present in the AMD. Survival after co-disposal of microorganisms found in AMD streams was assessed by culturing and phylogenetic methods. The test strain, *At. ferrooxidans*, was not culturable after mixing FA and AMD and genomic DNA could not be extracted. It can be concluded that microorganisms present in AMD cannot survive the mixing process, and are unlikely to survive in a VBNC form or even as naked genomic DNA.

To test the chemical and microbiological stability of the maturing solid phase, three pot trial experiments ([A] 100% solid phase, aerobic; [B] 100% solid phase, anaerobic and [C] 50:50 solid phase:soil, aerobic) were established. Genomic DNA could not be recovered from [A] and [B]. This might have been caused by the presence of toxic elements within the solid phase, the relatively short incubation period (10 weeks) or the presence of low numbers of microbial cells present in the solid phase. Low concentrations of DNA were recovered from pot samples [C] but the concentration of the DNA was too low (1-2 ng/µl) to be amplified.

To fully understand the FA-AMD co-disposal remediation system, more studies on the output phase are needed. The incubation period of the pot trials should be extended to determine whether a microbial community would develop over longer time periods. Qualitative and quantitative assessment of microbial community development in maturing FA-AMD solid phase samples could be investigated using:

1) Comparative analyses of microbial diversity using Denaturing Gradient Gel Electrophoresis (DGGE), coupled with phylogenetic analyses.
   - Using DGGE gel profiles the microbial diversity can be compared at different time intervals. Dominant phylotypes within the samples could then be identified, using 16S or 18S rDNA gene sequences.
2) Assessment of bacterial, archaeal and fungal diversity using sequence libraries.
   - PCR amplifications using universal bacterial, archaeal and fungal primers would identify the microbial diversity present in the maturing solid phase.
3) Group-specific phylogenetic analyses.
   - PCR amplifications using specific primers could identify specific organisms, such as sulfate reducing bacteria or methanogens present in the maturing solid phase.

These studies are currently being carried out by the ARCAM laboratory, University of the Western Cape.

The results obtained from this project and previous chemical studies, discussed in the first paragraph of this chapter, suggest that utilization of South African FA is an effective method for the treatment of coal mine derived AMD. Currently coal mining companies must choose between passive and active treatment technologies. Passive treatments such as wetlands are cost effective, but produce chemically unstable sediments (Skousen, 1997; Jage *et al*., 2001). Furthermore, the heavy metal content of the wetland sediments can exceed the legal standards for hazardous waste. Although active treatment technologies produces effluent water that meets water quality standards, it is more

expensive (Burgess and Stuetz, 2002). The neutralizing agent FA allows the hydration and precipitation of heavy metals and FA can be produced at minimal costs (Burgess and Stuetz, 2002; Petrik *et al*., 2003; Surender and Petrik, 2005). This process also facilitates the waste management of two environmentally unfriendly by-products, produced in the sector of the power generating industry.

References

Altschul, S.F., Madden, T., Schäffer, A.A., Zhang, J., Zhang, Z.W., Miller, W. and Lipman, D.J. (1997). Gapped BLAST and PSI-BLAST: a new generation of protein database search programs. *Nucleic Acids Research* **25**, 3389 – 3402.

Bacelar-Nicolau, P. and Johnson, D.B. (1999). Leaching of pyrite by acidophilic heterotrophic iron-oxidizing bacteria in pure and mixed cultures. *Applied and Environmental Microbiology* **65**, 585 – 590.

Baker, B.J. and Banfield, J.F. (2003). Microbial communities in acid mine drainage. *FEMS Microbial Ecology* **44**, 139 – 152.

Battaglia-Brunet, F., Dictor, M.C., Garrido, F., Crouzet, C., Morin, D., Dekeyser, K., Clarens, M. and Baranger, P. (2002). An arsenic (III)-oxidizing bacterial population: selection, characterization, and performance in reactors. *Journal of Applied Microbiology* **93**, 656 – 667.

Berthelet, M., Whyte, L.G. and Greer, C.W. (1996). Rapid, direct extractions of DNA from soils for PCR analysis using polyvinylpolypyrrolidone spin columns. *FEMS Microbiology Letters* **138**, 17 – 22.

Blake II, R.C., Shute, E.A. and Howard, G.T. (1994). Solibilization of Minerals by Bacteria: Electrophoretic mobility of *Thiobacillus ferrooxidans* in the presence of iron, pyrite, and sulfur. *Applied and Environmental Microbiology* **60**, 3349 – 3357.

Bond, B.L., Druschel, G.K. and Banfield, J.F. (2000). Comparison of acid mine drainage microbial communities in physically and geochemically distinct ecosystems. *Applied and Environmental Microbiology* **66**, 4962 – 4971.

Bond, P.L., Smriga, S.P. and Banfield, J.F. (2000). Phylogeny of microorganisms populating a thick, subaerial, predominantly lithotrophic biofilm at an extreme acid mine drainage site. *Applied and Environmental Microbiology* **66**, 3842 – 3849.

Bruynesteyn, A. (1989). Mineral biotechnology. *Journal of Biotechnology* **11**, 1 – 10.

Burgess, J.E. and Stuetz, R.M. (2002). Activated sludge for the treatment of sulphur-rich wastewaters. *Minerals Engineering* **15**, 839 – 846.

Coram N.J. and Rawlings, D.E. (2002). Molecular relationship between two groups of the genus *Leptospirillum* and the finding that *Leptospirillum ferriphilum* sp. nov. dominates South African commercial biooxidation tanks that operate at 40ºC. *Applied and Environmental Microbiology* **68**, 838 – 845.

Costello, C. (2003). Acid Mine Drainage: Innovative Treatment Technologies. For: U.S. Environmental Protection Agency, Office of Solid Waste and Emergency Response, Technology Innovation Office, Washington, DC, pp. 1 – 52.

Czurda, K.A. and Haus, R. (2002). Reactive barriers with fly ash zeolites for *in situ* groundwater remediation. *Applied Clay Science* **21**, 13 – 20.

Duquesne, K., Lebrun, S., Casiot, C., Bruneel, O., Personné, C., Leblanc, M., Elbaz-Poulichet, F., Morin, G. and Bonnefoy, V. (2003). Immobilization of arsenite and ferric iron by *Acidithiobacillus ferrooxidans* and its relevance to acid mine drainage. *Applied and Environmental Microbiology* **69**, 6165 – 6173.

Farelly, V., Rainey, F.A. and Stackebrandt, E. (1995). Effect of genome size and *rrn* gene copy number on PCR amplification of 16S rRNA genes from a mixture of bacterial species. *Applied and Environmental Microbiology* **61**, 2798 – 2801.

Fowler, T.A., Holmes, P.R. and Crundwell, F.K. (1999). Mechanism of pyrite dissolution in the presence of *Thiobacillus ferrooxidans*. *Applied and Environmental Microbiology* **65**, 2987 – 2993.

Fripp, J., Ziemkiewics, P.F. and Charkavork, H. (2000). Acid mine drainage treatment. In: EMRRP Technical Notes Collection. U.S. Army Engineer Research and Development Center, Vicksburg, MS, pp. 1 – 7.

Galtier, N., Gouy, M. and Gautier, C. (1996). SeaView and Phylo_win, two graphic tools for sequence alignment and molecular phylogeny. *Computer Applications in the Biosciences* **12**, 543 – 548.

Gitari, W.M., Somerset, V.S., Petrik, L.F., Key, D., Iwuoha, E. and Okujeni, C. (2003). Treatment of acid mine drainage with fly ash: Removal of major, minor, elements, SO_4 and utilization of the solid residues for wastewater treatment. *International ash utilization symposium*, Center for Applied Energy Research, University of Kentucky, pp. 1 – 23.

Hall, T.A. (1999). BioEdit: a userfriendly biological sequence alignment editor and analysis program for Windows 95/98/NT. *Nucleic Acids Symposium Series* **48**, 95 – 98.

Hallberg, K.B. and Johnson, D.B. (2003). Novel acidophiles isolated from moderately acidic mine drainage waters. *Hydrometallurgy* **71**, 139 – 148.

Harahuc, L., Lizama, H.M. and Suzuki, I. (2000). Selective inhibition of the oxidation of ferrous iron or sulfur in *Thiobacillus ferrooxidans*. *Applied and Environmental Microbiology* **66**, 1031 – 1037.

Hippe, H. (2000) *Leptospirillum* gen. nov. (ex Markosyan 1972), nom. re., including *Leptospirillum ferrooxidans* sp. nov. (ex markosyan 1972), nov. rev. and *Leptospirillum*. *International Journal of Systematic and Evolutionary Microbiology* **2**, 501 – 503.

Jage, C.R., Zipper, C.E. and Nobble, R. (2001). Factors affecting alkalinity generation by successive alkalinity-producing systems: Regression Analysis. *Journal of Environmental Quality* **30**, 1015 – 1022.

Johnson, D.B. (1995). Acidophilic Microbial Communities: Candidates for Bioremediation of Acidic Mine Effluents. *International Biodeterioration & Biodegradation* **35**, 41 – 58.

Johnson, D.B., Bacelar-Nicolau, P., Okibe, N., Yahya, A. and Hallberg, K.B. (2001). Role of pure and mixed cultures of gram-positive eubacteria in mineral leaching. (in) Ciminelli,V.T. and Garcia,O. Jr. (Eds.); Biohydrometallurgy: Fundamentals, technology and sustainable development, Elsevier, Amsterdam, Netherlands **11,** 461 – 470.

Johnson, D.B. and Hallberg, K.B. (2003). The microbiology of acidic mine waters. *Research in Microbiology* **154**, 466 – 473.

Johnson, D.B. and McGinnes, S. (1991). Ferric iron reduction by acidophilic heterotrophic bacteria. *Applied and Environmental Microbiology* **57**, 207 – 211.

Johnson, D.B. and Rang, L. (1993). Effects of acidophilic protozoa on populations of metal-oxidizing bacteria during the leaching of pyretic coal. *Journal of General Microbiology* **139**, 1417 – 1423.

Johnson, D.B., Rolfe, S., Hallberg, K.B. and Iversen, E. (2001). Isolation and phylogenetic characterization of acidophilic microorganisms indigenous to acidic drainage waters at an abandoned Norwegian copper mine. *Environmental Microbiology* **3**, 630 – 637.

Keller, L. and Murr, L.F. (1982). Acid-bacterial and ferric sulfate leaching of pyrite single crystals. *Biotechnology Bioenginering* **24**, 83 – 89.

Kelly, D.P. and Wood, A.P. (2000). Reclassification of some species of *Thiobacillus* to the newly designated genera *Acidithiobacillus* gen. nov., *Halothiobacillus* gen. nov. and *Thermithiobacillus* gen. nov. *International Journal of Systematic and Evolutionary Microbiology* **50**, 511 – 516.

Kishimoto, N., Kosaka, Y. and Tano, T. (1991). *Acidobacterium capsulatum* gen. nov., sp. nov.: an acidophilic chemoorganotrophic bacterium containing menaquinone from acidic mineral environment. *Current Microbiology* **22**, 1 – 7.

Kishimoto, N., Kosako, Y., Wakao, N., Tano, T. and Hiraishi, A. (1995). Transfer of *Acidiphilium facilis* and *Acidiphilium aminolytica* to the genus *Acidocella* gen. nov., and emendation of the genus *Acidiphilium*. *Systematic and Applied Microbiology* **18**, 85 – 91.

Madigan, M.T., Martinko, J.M. and Parker, J. (2000). Brock Biology of Microorganisms. Eighth Edition. *Prentice Hall International, Incorporation*, New Jersey, pp. 576 – 578.

Martin-Laurent, F., Philippot, L., Hallet, S., Chaussod, R., Germon, J. C., Soulas, G. and Catroux, G. (2001). DNA extraction from soils: Old bias for new microbial diversity analysis methods. *Applied and Environmental Microbiology* **67**, 2354–2359.

Mustin, C., Berthelin, J., Marion, P. and De Donato, P. (1992). Corrosion and electrochemical oxidation of a pyrite by *Thiobacillus ferrooxidans*. *Applied and Environmental Microbiology* **58**, 1175 – 1182.

Olson, G.J. (1991). Rate of pyrite bioleaching by *Thiobacillus ferrooxidans*: Results of an interlaboratory comparison. *Applied and Environmental Microbiology* **57**, 642 – 644.

Petrik, L.F., White, R.A., Klink, M.J., Somerset, V.S., Burgers, C.L. and Fey, M.V. (2003). Utilization of South African fly ash to treat acid coal mine drainage, and production of high quality zeolites from the residual solids. *International ash utilization symposium*, Center for Applied Energy Research, University of Kentucky, pp. 1 – 26.

Prescott, L.M., Harley, J.P. and Klein, D.A. (1999). Microbiology Forth Edition. *The McGraw-Hill Companies, Incorporation*, New York, pp. 181.

Ram, R.J., VerBerkmoes, N.C., Thelen, M.P., Tyson, G.W, Baker, B.J., Blake II, R.C., Shah, M., Hettich, R.L. and Banfield, J.F. (2005). Community proteomics of a natural microbial biofilm. *Science* **308**, 1915 – 1920.

Rawlings, D.E. (2002). Heavy metal mining using microbes. *Annual Review of Microbiology* **56**, 65 – 91.

Razzel, W.E. and Trussel, P.C. (1963). Isolation and properties of an iron-oxidizing *Thiobacillus*. *Journal of Bacteriology* **85**, 595 – 603.

Reysenbach, A.L. and Pace, N.R. (1995). Reliable amplification of hyperthermophilic Archaeal 16S rRNA genes by the Polymerase Chain Reaction. In: Robb FT, Place A. R. (eds) *Archaea*: A Laboratory Manuel – Thermophiles. *Cold Spring Harbour Laboratory Press*, New York, pp. 101 – 106.

Rohwerder, T., Gehrke, T., Kinzler, K. and Sand, W. (2003). Bioleaching review part A: Progress in bioleaching: fundamentals and mechanisms of bacterial metal sulfide oxidation. *Applied Microbiology and Biotechnology* **63**, 239 – 248.

Sand, W. (1989). Ferric iron reduction by *Thiobacillus ferrooxidans* at extreme low pH-values. *Biogeochemistry* **7**, 195 – 201.

Schippers, A. and Sand, W. (1999). Bacterial leaching of metal sulfides proceeds by two indirect mechanisms via thiosulfate or via polysulfides and sulfur. *Applied and Environmental Microbiology* **65**, 319 – 321.

Selenska-Pobell, S., Kampf, G., Hemming, K., Radeva, G. and Satchanska, G. (2001). Bacterial diversity in soil samples from two uranium waste piles as determined by rep-APD, RISA and 16S rDNA retrieval. *Antonie Van Leeuwenhoek* **79**, 149 – 161.

Simmons, S. and Norris, P. R. (2002). Acidophiles of saline water at thermal vents of Vulcano, Italy. *Extremophiles* **6**, 201 – 207.

Singer, P.C. and Stumm, W. (1970). Acidic mine drainage, the rate determining step. *Science* **167**, 1121 – 1123.

Skousen, J. (1997). Overview of passive systems of treating acid mine drainage. *Green Lands* **27**, 34 – 43.

Somerset, V.S. (2003). The preparation and characterization of high capacity ion exchange adsorbents made by co-disposal of fly ash and acid mine drainage for their possible use in electrochemical systems for water purification. M.Sc. Thesis. University of the Western Cape. Cape Town, South Africa, pp. 2 – 10.

South Africa Country Analysis Briefs. (2005). Energy Information Administration, pp. 1 – 12.

Styszko-Grochowiak, K., Golas, J., Jankowski, H. and Kozinski, S. (2004). Characterization of the coal fly ash for the purpose of improvement of industrial on-line measurement of unburned carbon content. *Fuel* **83**, 1847 – 1853.

Sugio, T.Y., Tsujita, K.I. and Tano, T. (1990). Reduction of cupric ions with elemental sulfur by *Thiobacillus ferrooxidans*. *Applied and Environmental Microbiology* **56**, 693 – 696.

Surender, D. and Petrik, L.F. (2005). Development of a Co-disposal Protocol for the neutralization and amelioration of acid mine drainage with fly ash. *International ash utilization symposium*, Center for Applied Energy Research, University of Kentucky, pp. 1 – 13.

The American Heritage® Dictionary of the English Language. Fourth Edition. (2000). *Houghton Mifflin Company*, Boston.

The Columbia Encyclopedia. Sixth Edition. (2001-04). *Columbia University Press*, New York.

The Water Wheel. (2003). Mine Water Treatment. *South African Water Research Commision* **2**, 6 – 8.

Thompson, J.D., Gibson, T.J., Plewniak, F., Jeanmougin, F. and Higgins, D.G. (1997). The ClustalX windows interface: flexible strategies for multiple sequence alignment aided by quality analysis tools. *Nucleic Acids Research* **24**, 4876 – 4882.

Tyson, G.W., Chapman, J., Hugenholtz, P., Allen, E.E., Ram, R.J., Richardson, P.M., Solovyev, V.V., Rubin, E.M., Rokhsar, D.S. and Banfield, J.F. (2004). Community structure and metabolism through reconstruction of microbial genomes from the environment. *Nature* **428**, 37 – 43.

Tyson, G.W., Lo, I., Baker, B.J., Allen, E.E., Hugenholtz, P. and Banfield, J.F. (2005). Genome-directed isolation of the key nitrogen fixer *Leptospirillum ferrodiazotrophum* sp. nov. from an acidophilic microbial community. *Applied and Environmental Microbiology* **71**, 6319 – 6324.